Response to comments of Referee 1.

As a general point, we agree that PMF/ME-2 analysis was probably not a perfect representation of the aerosol, however we argue that the factorisation given represents a 'best estimate' based on the testing and validation work performed. We consider that, while BBOA concentrations could be mixed with other OA sources implying a decrease on BBOA concentrations, the represents the best estimate of the temporal trend biomass burning OA emissions. This is supported by the good correlation BBOA shows with b_{abs_470wb} r2=0.880. Thus we consider BBOA time series to be accurate enough to determine primary and secondary PON concentrations.

Through discussions outside of this review, we have considered that the term Particulate Organic Nitrate (PON) is not the most appropriate as this could include nitro compounds in addition to organic nitrates. Hence, we have decided to refer to the acronym as Particulate Organic Oxides of Nitrogen (PON) which include both nitrate and nitro organic compounds. Furthermore, because the chemistry community do not strictly consider these compounds primary, the term 'primary' here should include the qualifier in that it is not necessarily produced in the fire, but on a short enough time scale that its temporal trend is indistinguishable from the actual primary emissions, so is therefore considered 'primary' within the receptor model.

Comments from referee are in blue and response from co-authors is in black.

Major comments.

1. PMF results.

It has been challenging to perform source apportionment on a dataset including a special event with high concentrations. This study takes an important step to address this issue. However, the PMF results are still not satisfactory. My major concern is that all OA factors show significant increase during the biomass burning event (Figure 5 and 6). LV-OOA increases by ~30 μg m-3. Since fresh biomass burning unlikely contribute to LV-OOA, the increase in LV-OOA suggests PMF artifacts. The COA and HOA increase by ~8 μg m-3 and ~20 μg m-3 during the biomass burning, respectively. These enhancement magnitudes cannot be explained by the inversion at night. The enhanced concentrations of LV-OOA, COA, and HOA during the biomass burning event are likely interference from biomass burning.
Using the suggested two-step approach, a clean BBOA factor still cannot be resolved. For example, BBOA_1 is a mixed factor between LV-OOA and BBOA. Have the authors tried PMF2 solver on the whole dataset? Including the biomass burning event would be useful to get a clear BBOA factor, which helps to identify the BBOA concentration during the non-biomass burning period. However, the disadvantage of this method is that the concentrations of all OA factors would falsely decrease during the biomass burning.

We agree that during bonfire night, LV-OOA, COA and HOA may be mixed with BBOA concentrations. We mention in section 4.1 that this would be the case. Conclusions will be modified mentioning that even when using the methodology of first analysing the period before and after bonfire night and then analyse the bonfire night period, it was not possible to completely separate the OA sources. We run PMF and ME-2 for the whole dataset (test1). However, when we compared solutions from different tests, analysing first the period without bonfire emissions and then the bonfire night event, was best way to do source apportionment.

The following paragraph has been added to the end of section 4.1 OA source apportionment during bfo event:

Here we show the importance of performing OA source apportionment using different approaches in order to identify the best way to deconvolve OA sources. PMF and ME-2 source apportionment tools could not completely deconvolve OA sources during the bfo event. However, due to the high correlation between for b_{abs_470wb} and BBOA_2 (r^2 = 0. 880) we consider that while BBOA_2 might not represent the total OA concentrations from the bonfire night event, it does represent the trend of OA emmited from the biomass burning.

The authors have done careful evaluation on PMF results. PMF results from two different tests (test 2 and test 2_ON) are presented, but the PMF results are different. This causes many confusions. For example, why does the mass spectrum of BBOA change between test 2 and test 2_ON (i.e., BBOA-2 vs BBOA)? Why are two BBOA factors are resolved in test 2, but only one BBOA factor in test 2_ON? Why is SV-OOA only resolved in test 2, but not in test 2_ON? I suggest the authors to present only the most reasonable/best solution in the manuscript to avoid confusion.

We agree two solutions in the manuscript to be confusing. The manuscript has been edited, leaving only one solution on the main manuscript (Test2_ON). The other solution has been moved to the appendix, as one of the objectives of this paper is to assess ME-2 under different tests in order to study its performance.

This paragraph has been added to section 3.3 OA source apportionment:

Test2_ON was the optimal 'best estimate' solution, a brief description is given here after being compared to the other tests (Section S7.2 in supplement). From this analysis, test2 was the best way to deconvolve OA sources, with the lowest parameters analysed: residuals, Q/Qexp values and Chi square. After modifying the fragmentation table, Test2_ON still shows a good performance with low parameters (Fig. S6-S8). Refer to section S7 in supplementary material for detailed information about source apportionment strategy and analysis performed to determine the optimal solution.

2.

(1) The most important issue is that the r2 values in the manuscript do not match those in table 1.

The r2 values on table 1 are the correct r2 values. The values mentioned on the paragraph were not updated from a previous version. r2 values have been updated.

(2) What's the rationale behind eqn. 6? Why is the partial slope used? In MLR3, there is no sPON_ME2. Then how is the light-absorption of sPON_ME2 evaluated?

We have expanded the explanation of the multilinear equation. There is sPON_ME2 in MLR3, the following two paragraphs have been added to explain equation 6.

$$b_{abs\_470wb} = A + B*x1 + C*x2 \quad (6)$$

When the parameter s"D" and x3 are used it means a trilinear regression was performed. MLR1 x1=BBOA, x2=PON. MLR2 x1=BBOA_2, x2=PON. MLR3 x1= BBOA_2, x2=sPON_ME2, x3=LVOOA in HSC and x3= pPON in bfo. A is the origin and the partial slopes B, C and D represent the contribution of x1 ,x2 and x3 to b_{abs_470wb}, respectively.

As used in previous studies (Elser et al., 2016;Reyes-Villegas et al., 2016), multilinear regression analysis allows to determine the relationship between one parameter and two or more variables. Here we are analysing the partial slopes and origin to determine the correlation of babs_470wb with the other variables.

(3) In the abstract, it is stated that LV-OOA absorb light at 470nm over that of black carbon. Where is the justification for this conclusion?

Sorry to be ambiguous, the abstract has been edited as follows:

Our results suggest that sPON_ME2 does not absorb light at 470 nm while pPON_ME2 and LVOOA absorb light at 470 nm.

(4) Line 278, the authors state that after modifying the fragmentation table, the correlation between babs_470wb and BBOA is improved. I wonder if the improvement is mainly because that there are only one BBOA is resolved in test 2_ON, but two BBOA factors in test 2? In other words, is the improved correlation simply due to that modifying the fragmentation table somehow helps to separate the BBOA factor? What's the r2 between babs_470wb and the sum of BBOA and BBOA_1 in test 2?

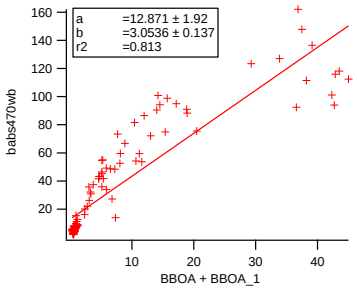

We still consider OA source apportionment improves after modifying the fragmentation table. During the bonfire night r2 values between b_{abs_470wb} and BBOA is 0.839 before the modification and 0.880 after the modification, while r2 =0.813 is obtained between b_{abs_470wb} and the sum of BBOA+BBOA_1. The r2 = 0.813 will be mentioned in the manuscript

(5) Line 374, the authors need to be cautious that not all organic nitrates can absorb light. Most identified light-absorbing organic nitrate are nitro aromatic compounds (Lin et al., 2016; Mohr et al., 2013).

We have decided to change our definition of PON from "particulate organic nitrate" to "particulate organic oxides of nitrogen" which will involve both nitro and nitrate organic compounds.

3. The separation of primary PON (pPON) and secondary PON (sPON).
(1) How do the authors identify pPON and sPON? In Figure 6, the sPON_ME2 has more evident signal at m/z 30 than pPON. What does the mass spectrum of organics that associate with sPON look like? Where are the organic signals associated with pPON_ME2 from? Fresh biomass burning? More discussions regarding pPON_ME2 and sPON_ME2 are required.

The following paragraph has been added to the end of the section 3.3 OA source apportionment:

These two PON factors may have different sources; one may be secondary (sPON_ME2) as it follows the trend of LVOOA concentrations (Fig. 5.a) and the other primary (pPON_ME2) which has similar trend as BBOA (Fig. 5.b). Further details about pPON_ME2 and sPON_ME2 nature will be explored in section 4.2.

Moreover, the following paragraph has been added to the end of section 4.3:

During the bfo event, pPON_ME2 showed high r2 values with carbon monoxide (0.78) as well as hydrogen cyanide (0.77), Methylformamide (0.65) and Dimethylformamide (0.63) which are typical primary pollutants related to combustion processes [(Borduas et al., 2015) and references therein]. sPON_ME2 showed low correlations with ClNO2 (0.52) and ClNO3 (0.53). High r2 values were also observed during LC episode between ClNO2 - ClNO3 and LVOOA (0.67 - 0.66) and sPON (0.74 - 0.69) proving their secondary origin.

(2) The authors use two methods to differentiate pPON and sPON. However, there are discrepancies in the results (Figure 7 vs. 8). For example, pPON_ME2 decreases slower than BBOA in Figure 8. Could the authors directly compare the results from these two methods (i.e., scatter plot)?

This information will be added to supplement

Two methods have been used to determine primary and secondary PON. In the following plots we can see primary PON comparison has a good correlation with a pearson value of 0.7 while secondary PON comparison shows a different behaviour between them.

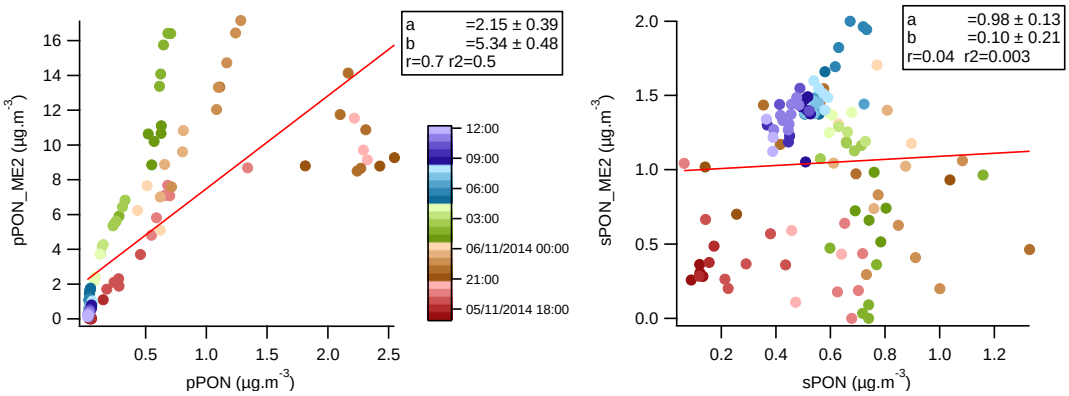

Figure S13: PON comparison for the two methods used.

(3) Previous studies have attempted to run PMF analysis on combined organic and nitrate mass spectra (Sun et al., 2012; Xu et al., 2015). The authors should compare to other literature.

This paragraph has been added to methodology in the section were we describe ME-2 PON analysis:

Previous studies have quantified PON concentrations from AMS-PMF analysis to both rural and urban measurements (Sun et al., 2012;Hao et al., 2014;Xu et al., 2015;Zhang et al., 2016).

This paragraph has been added to section 4.2 PON Primary/secondary:

Primary and secondary sources of PON have been previously identified from AMS-PMF analysis; Hao et al. (2014) identified PON to be secondary of nature, produced from the interaction between forest and urban emissions, while Zhang et al. (2016) determined PON to be related to primary combustion sources.

Minor Comments

1. Line 68. It should be "Ng et al., 2017".

The citation has been edited.

2. Line 212. What's the NO2+/NO+ value of organic nitrate used in this study? This information should be mentioned in the main text.

The following paragraphs have been edited in section 2.2.2 Particulate Organic Oxides of Nitrogen (PON):

Equation 5 calculates the PON fraction (X_{PON}), using the signals at m/z 30 and m/z 46 to calculate m/z ratios 46:30 from AMS measurements (R_{meas}), from ammonium nitrate calibrations (R_{cal}), and from organic nitrogen (R_{ON}) to quantify PON concentrations.

$$X_{PON} = \frac{(R_{meas}-R_{Cal})(1+R_{ON})}{(R_{ON}-R_{cal})(1+R_{meas})} \quad (5)$$

Where ratios from ammonium nitrate calibrations Rcal = 0.5; Rmeas = m/z 46:30 ratio from measurements; m/z 46:30 ratio from ON RON = 0.1, Following Kostenidou et al. (2015) consideration, R_{ON} = 0.1 was calculated as the minimum m/z 46:30 ratio observed. RON value of 0.1 has been used in previous studies (Kiendler-Scharr et al., 2016;Tiitta et al., 2016).

$$PON = X_{PON} * NO_3^- \quad (6)$$

Finally, equation 6 calculates PON concentrations [µg.m-3] where NO3- is the total nitrate measured by the cToF-AMS.

3. Line 227. The mass spectrum of factor 4 is very similar to that of SV-OOA in step a. Then how do the authors justify "SV-OOA" in step a?

This figure has been moved to the appendix A. In this figure, we consider factor 4 mass spectra to be SVOOA in both (a) and (b).

4. Line 392, please cite Washenfelder et al. (2015), which showed that biomass burning OA is light absorbing.

The citation has been added to the manuscript.

Response to comments of Referee 2.

Comments from referee are in blue and response from co-authors is in black.

Major comments.

Quantification of PON from biomass burning using a CToF-AMS: The m/z 46:30 ratio is used for the quantification of PON, which is based on a method done by Farmer et al 2010 that used an HR-AMS and did not include any biomass burning emissions. The large fraction of OA from biomass burning certainly will produce a large CH2O+ contribution and will make the quantification of PON very different compared to the Farmer et al paper. On page 7 line 250 the authors say that the m/z 30 interference is likely small, but this might be very different in biomass burning and needs to be shown or given a reference. In addition it is written on page 6 line 206 that the interference of CH2O+ is discussed in section 3.4.1, but no such section exists in the paper. So it is not clear, how the authors deal with the m/z 30 interference and how large the uncertainty or error estimate on the quantification of PON is. In addition in the later section, where the primary versus secondary PON is discussed, it is certainly possible that the m/z 30 interference is different as the composition changes during the later part of the night, when the authors claim that they observed secondary PON. A section needs to be added, where the interference is clearly explained and the effect needs to be quantified. This should result in an uncertainty range for the m/z 30:46 ratio and error estimate for PON. All of this should be added to the instrumentation section, where there needs to be a description of the AMS added as well that includes a discussion on the calibration for NH4NO3 and, if available, for PON compounds. Here it should be made clear what m/z 30:46 ratio NH4NO3 has in this particular instrument? The resulting error estimate needs to be taken into account for the following discussions.

Section 2.2.2 in methods has been edited as follows:

2.2.2 Particulate Organic Oxides of Nitrogen (PON)

Concentrations of PON were calculated following the method proposed by Farmer et al. (2010) and the considerations used by Kiendler-Scharr et al. (2016). This method has been previously used in studies looking at aerosols from biomass burning (Tiitta et al., 2016;Zhu et al., 2016;Florou et al., 2017). Equation 5 calculates the PON fraction (X_{PON}), using the signals at m/z 30 and m/z 46 to calculate m/z ratios 46:30 from AMS measurements (R_{meas}), from ammonium nitrate calibrations (R_{cal}), and from organic nitrogen (R_{ON}) to quantify PON concentrations.

$$X_{PON} = \frac{(R_{meas} - R_{Cal})(1+R_{ON})}{(R_{ON} - R_{cal})(1+R_{meas})} \quad (5)$$

Where ratios from ammonium nitrate calibrations R_{cal} = 0.5; R_{meas} = m/z 46:30 ratio from measurements; m/z 46:30 ratio from ON R_{ON} = 0.1, Following Kostenidou et al. (2015) consideration, R_{ON} = 0.1 was calculated as the minimum m/z 46:30 ratio observed. R_{ON} value of 0.1 has been used in previous studies (Kiendler-Scharr et al., 2016;Tiitta et al., 2016).

$$PON = X_{PON} * NO_3^- \quad (6)$$

Finally, equation 6 calculates PON concentrations [$\mu g.m^{-3}$] where NO_3^- is the total nitrate measured by the cToF-AMS. The method proposed by Farmer et al. (2010) is based on HR-ToF-AMS measurements were m/z 30 represents NO^+ ion and m/z 46 NO_2^+ ion while the cToF-AMS gives unit mass resolution mass spectra information, hence, there is the possibility to have interference of CH_2O^+ ion at m/z 30. However, when analysing mass spectra from previous laboratory and ambient studies using HR-ToF-AMS to investigate biomass burning emissions, we can confirm that the signal of CH_2O^+ at m/z 30 is low compared to signals at m/z's 29 and 31, while in this study m/z 30 is the main signal (Fig. 5.c). Hence, in this study an interference of CH_2O^+ at m/z 30 is unlikely and if there were any interference of CH_2O^+ it would be negligible. Table S1 in

supplement shows m/z 30/29 and 30/31 from previous laboratory and ambient studies investigating biomass burning emissions.

Another possible interference would be the presence of mineral nitrates at m/z 30 (e.g. KNO_3 and $NaNO_3$). However, mineral nitrate salts tend to be large particles (Allan et al., 2006;Chakraborty et al., 2016) and also have low vaporisation efficiency (Drewnick et al., 2015), which makes it unlikely to be measured by the AMS in large quantities.

Table S1. CH_2O^+ signals at m/z 29, 30 and 31 from HR-ToF-AMS data of previous studies. Comparison of m/z ratios 30/29 and 30/31 with values found in this study.

	Reference	30/29	30/31	m/z 29	m/z 30	m/z 31	Notes
ambient	This study	4.38	35.00	0.08	0.35	0.01	sPON_ME2
		1.42	8.50	0.06	0.09	0.01	pPON_ME2
	(Aiken et al., 2010)	0.16	0.32	0.05	0.008	0.025	pine burn
		0.20	0.45	0.045	0.009	0.02	BBOA Mex
	(Collier et al., 2016)	0.25	0.56	4	1	1.8	Ground plume
		0.20	0.60	3	0.6	1	Ground plume
		0.23	0.67	3.5	0.8	1.2	aircraft plume
		0.25	1.25	4	1	0.8	aircraft plume
	(Zhou et al., 2017)	0.18	0.88	8	1.4	1.6	no bb
		0.32	0.95	6	1.9	2	bb inf
		0.30	0.90	6	1.8	2	bb plm
Laboratory-based	(He et al., 2010)	0.25	0.75	0.06	0.015	0.02	Fir (diluted/cooled)
		0.21	0.68	0.07	0.015	0.022	pine burn
		0.20	0.56	0.05	0.01	0.018	Willow
		0.30	0.90	0.06	0.018	0.02	Wattle
		0.30	0.90	0.06	0.018	0.02	SugaCaneLeave
		0.30	0.08	0.05	0.015	0.2	Rice Straw
	(Heringa et al., 2011)	0.25	0.67	4	1	1.5	poa
		0.25	0.50	4	1	2	5h aging
	(Ortega et al., 2013)	0.15	0.50	13	2	4	start (oak)
		0.20	0.50	50	10	20	aged (oak)
		0.04	0.05	250	10	220	start (pine)
		0.07	0.10	270	20	200	aged (pine)
	(Corbin et al., 2015b)	0.20	0.80	4	0.8	1	start
			0.83		0.05	0.06	flaming
	(Corbin et al., 2015a)		0.50		0.01	0.02	Filtered and Oxid
			0.50		0.01	0.02	Oxidized
		0.25	0.50	0.04	0.01	0.02	Primary
	(Bruns et al., 2015)	0.43	6.00	0.07	0.03	0.005	OH and UV exp.
		0.34	1.00	0.065	0.022	0.022	OH and UV exp.
		0.40	1.00	0.045	0.018	0.018	OH and UV exp.
		0.34	1.00	0.065	0.022	0.022	OH and UV exp.
		0.40	1.00	0.045	0.018	0.018	OH and UV exp.
		0.23	1.00	0.048	0.011	0.011	OH and UV exp.
		0.20	1.00	0.04	0.008	0.008	OH and UV exp.
		0.25	1.00	0.048	0.012	0.012	OH and UV exp.

These paragraphs have been added to describe Table S1 in the supplement.

Table S1 shows CH_2O^+ signals at m/z's 29, 30, and 31 from HR-ToF-AMS studies. It is possible to observe the low CH_2O^+ contribution to m/z 30 with 30/29 ratios between 0.01-0.40. The high values of 0.4 – 6 were observed when exposing aerosols to OH and UV. We can also see that 30/31 30/29 ratios do not show variations during and after biomass burning events or during fresh and aged emissions (Ortega et al., 2013;Corbin et al., 2015a;Corbin et al., 2015b), suggesting there is not substantial CH_2O^+ variability over the biomass burning process.

In this study, a large contribution of m/z 30 signal to the mass spectra was observed with both sPON and pPON with 30/29 ratios (4.38 and 1.42 respectively) and 30/31 ratios (35.0 and 8.5 respectively) higher than unity. Showing that a CH_2O^+ interference at m/z30 would be unlikely.

For biomass burning the fragmentation tables need to be modified, which the authors do later in the paper. It does not make sense to me to run PMF on not-corrected data as was done in Section 3.3, when you know you are using incorrect data.

We agree on showing both solutions in the main manuscript is confusing. The PMF solution without modifying the fragmentation table has been moved to the appendix. Part of this paper is to explore different ways to run ME-2 and evaluate its performance under different conditions, hence we consider important to show this solution on the appendix.

The section on the FragPanel modification is very specific to AMS users and all the three bullet points cannot be understood by anybody else without explaining all the abbreviations and acronyms. Especially sentences like on page 7 line 238: time series of PON:mz30 were calculated with the equation PON:mz30=PON/mz30, where PON=m/z 46:30. This makes mathematically no sense. Again all of this need to be included in the instrument section together with the quantification of PON and clearly will increase the already large uncertainty in the PON quantification during the biomass burning event.

The following paragraphs have been added to the end of section 2.2.3 Multilinear engine 2 (ME-2):

PON may exhibit covariance with other types of OA, thus their inclusion in the source apportionment analysis may give a more complete factorisation and highlight their co-emission with other OA types. Therefore, a different experiment was designed by modifying the fragmentation table, through the AMS analysis toolkit 1.56, in order to identify a PON source. The fragmentation table contains the different chemical species measured by the AMS, with each row representing m/z for specific species and where the user can define peaks that exist in each species' partial mass spectrum and their dependency on other peaks (Allan et al., 2004). The following steps were performed to modify the fragmentation table:

- Time series of a new ratio named RON_30 is calculated by RON_30 = PON/mz30, were PON is the time series calculated in section 2.2.2 and mz30 is the time series of the signal at m/z=30 measured by the AMS.
- Using the AMS analysis toolkit; the fragmentation table is modified, in the column frag_Organic at the m/z 30, by multiplying RON_30*30. See figure S4 in supplement for a screenshot of the fragmentation table.
- PMF inputs are generated to be used in SoFi software.

Figure S4 has been added to the supplement to show how fragmentation table has been modified.

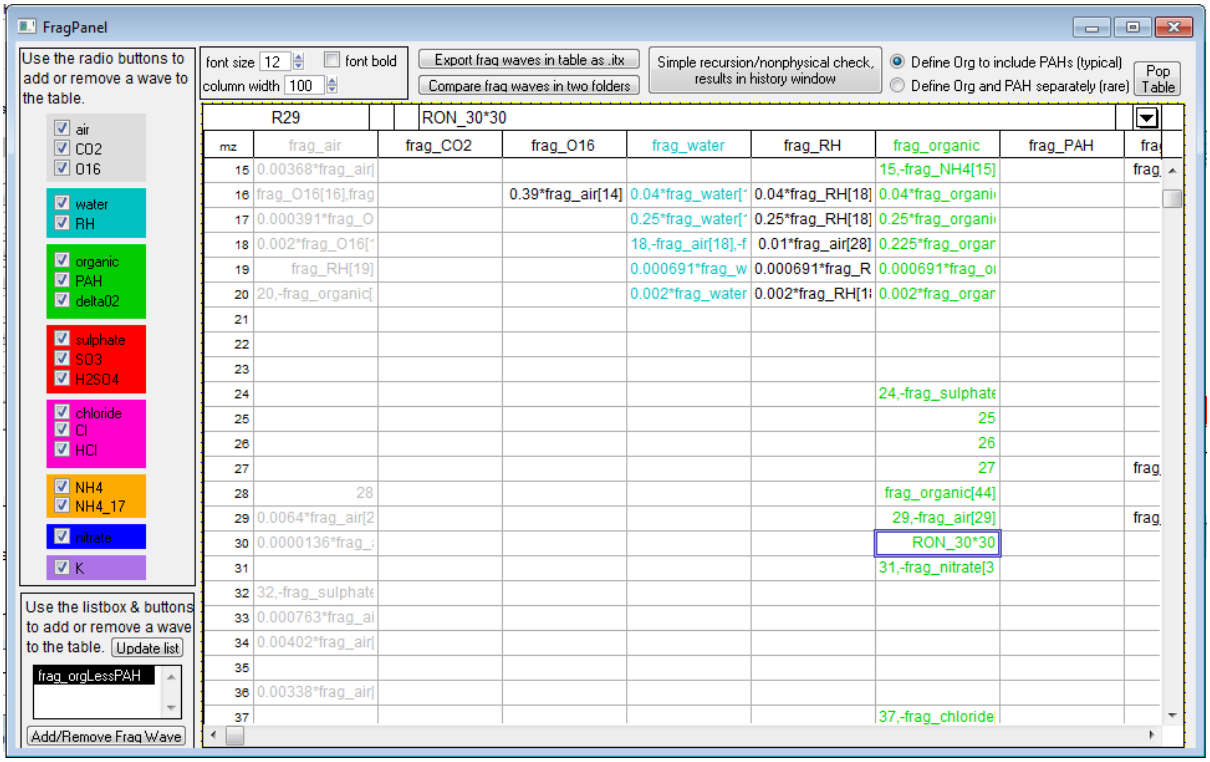

Figure S4: Modifying fragmentation table to add PON to PMF analysis.

The description of PMF and the ability of PMF to resolve the biomass burning event:

In my opinion, PMF is pushed way too far in this manuscript given the quality of the data. It is well known that PMF has difficulties to resolve large individual peaks and this becomes very clear in this paper as well.

As mentioned to Referee 1, we agree that, during bonfire night, LV-OOA, COA and HOA may be mixed with BBOA concentrations. We mentioned in section 4.1 that this would be the case. Conclusions will be modified mentioning that even when using the methodology of first analysing the period before and after bonfire night and then analyse the bonfire night period, it was not possible to completely separate the OA sources. However, we consider that, while BBOA concentrations would be mixed with other OA sources implying a decrease on BBOA concentrations, the actual BBOA trend remains and BBOA factor is considered to be representative of biomass burning OA emissions. This is supported by the good correlation BBOA shows with b_{abs_470wb} r^2=0.880, a marker of emissions from biomass burning. Thus we consider BBOA time series to be accurate enough to determine primary and secondary PON concentrations.

The following paragraph has been added to the end of section 4.1 OA source apportionment:

Here is shown the importance of performing OA source apportionment using different approaches in order to identify the best way to deconvolve OA sources. PMF and ME-2 source apportionment tools could not completely deconvolve OA sources during the bfo event. However, due to the high correlation between for b_{abs_470wb} and BBOA_2 (r^2 = 0. 880) we consider that while BBOA_2 might not represent the total OA concentrations from the bonfire night event, it does represent the trend of OA emmited from the biomass burning.

First of all this paper is clearly tailored to the AMS community, but it should at least be somewhat understandable to anybody else, especially when some of the main findings are related to the absorption of PON. None of the factors that are used such as HOA, COA or LVOOA are explained anywhere or even a reference given. What are those factors, how are they characterized, how do they relate to any of the other measured tracers and how do the ones determined in this manuscript compare to the AMS data base?

We have added a more understandable description of the OA sources with their respective references, The following paragraph has been edited in the section 3.3 OA source apportionment:

Two steps were involved in Test2_ON: in step a, PMF/ME-2 were run for the event before and after the bonfire night (named as not bonfire event, nbf). In Step b, mass spectra from the solution identified in step a were used as TP, to analyse the bonfire-only (bfo) event. Finally, both solutions (nbf and bfo) were merged for further analysis. Different OA sources were identified in Test2_ON (Fig. 5), five sources were identified during nbf event: biomass burning OA (BBOA), hydrocarbon-like OA (HOA), cooking OA (COA), secondary particulate organic oxides of nitrogen (sPON_ME2) and low volatility OA (LVOOA). These sources are identified by characteristic peaks at their mass spectrum; BBOA, which is generated during the combustion of biomass, has a peak at m/z 60, related to levoglucosan (Alfarra et al., 2007); HOA, related to traffic emissions, presents high signals at m/z 55 and m/z 57 typical of aliphatic hydrocarbons (Canagaratna et al., 2004); COA, emitted from food cooking activities, is similar to HOA with a higher m/z 55 and lower m/z 57 (Allan et al., 2010;Slowik et al., 2010;Mohr et al., 2012); LVOOA, identified as a secondary organic aerosol, has a high signal at m/z 44 dominated by the CO_2^+ ion (Ng et al., 2010); sPON_ME2 has a strong signal at m/z 30 and it has been identified to be secondary as it follows the same trend as LVOOA (Figure 5.a). In the case of the bfo event six different sources were identified: BBOA, HOA, COA, LVOOA and two factors with peaks at m/z30, which is related to PON (Sun et al., 2012). These two PON factors may have different sources; one may be secondary (sPON_ME2) and the other primary (pPON_ME2) which has similar trend as BBOA (Fig. 5.b). Further details about pPON_ME2 and sPON_ME2 nature will be explored in section 4.2.

The next issue is that PMF was done in many different ways in this manuscript, many tests were performed and a lot of these tests were subsequently discarded. So why do you describe all the tests that have not worked. As it is written, this is very confusing and really hard to follow. Furthermore, two different PMF tests were actually used in the manuscript and they are very clearly different and the results that fit the story the best were used for no apparent reason. Even the number of BBOA factors changes between the two tests.

One of the objectives of this paper is to explore different ways to perform source apportionment, hence we consider important to mention the different tests perform. However, we agreed that mentioning both solutions in the main text is confusing. Hence, we have modified the manuscript by only explaining in the main text the optimal solution (Test2_ON) and moving the other solution to the appendix.

It is very clear that PMF, even in the way as done here with separating the biomass burning event from the rest of the time series, cannot resolve the single event. In Figure 6 the combined increase of LVOOA, COA, and HOA is about twice as large as the combined BBOA_2, sPON_ME and pPON_ME signals. One might argue that during bonfire night activities such as cooking and traffic might increased as well, but certainly not to such large extents. Especially the LVOOA signal, which is larger than the BBOOA signal, has to be from biomass burning as well. So it seems that the interferences in the biomass burning event are larger than the BBOA signal itself.
Given this large uncertainty and interferences on the PMF results, it seems clearly a step too far to try to separate sPON from pPON with two different methods that have large uncertainties and are not even fully consistent with each other. The I-CIMS measures some primary and secondary ON tracers, some of which are specific to biomass burning such as nitroaromatics, why have those measurements not been used to correlate with the sPON signal? It is not clear from the text on page 9, what compounds from the I-CIMS have actually been used, except some of the inorganic tracers.

This is the correct table, which is in the supplement:
Table S4: R^2 values between OA factors and CIMS measurements.

		BBOA					COA				sPON				LVOOA				pPON
Formula	Name	ALL	HSC	LC	bfo	WL	ALL	LC	bfo	WL	ALL	LC	bfo	WL	ALL	LC	bfo	WL	bfo
C4H6O2	methacrylic acid	0.89			0.92	0.53	0.64		0.77	0.48					0.78		0.82		0.52
C3H4O2	Acid_Acrylic	0.85			0.90	0.65	0.62		0.70	0.43				0.48	0.79		0.88		
H2COH2O	methylhydroperoxide	0.78			0.90		0.54		0.69						0.66		0.85		
C6H6O	Phenol	0.89			0.89		0.59		0.73						0.75		0.73		0.57
C7H6O2	Benzoic acid	0.89		0.57	0.89	0.86	0.65		0.83	0.45		0.71		0.73	0.67	0.72	0.64	0.58	0.57
C2H5NO	Methylformamide	0.88			0.89	0.47	0.61		0.79						0.65		0.67	0.56	0.65
C2H3NO	Methyl isocyanate	0.89	0.49	0.44	0.89	0.71	0.55		0.66					0.50	0.85		0.88		
C5H10O2	Pentanoic acid	0.77			0.87		0.60		0.76						0.54		0.66		
HNO2	nitrous acid	0.81			0.86	0.66	0.59		0.84					0.57	0.61		0.66		0.70
CH2O2	formic acid	0.52			0.86				0.62						0.58		0.88		
C3H7NO	Dimethylformamide	0.80			0.85		0.59		0.76						0.56		0.63	0.60	0.63
C3H6O2	propionic acid	0.87		0.67	0.85	0.72	0.53	0.45	0.62			0.41		0.67	0.78		0.78	0.63	
C2H5N3O2	C2H5N3O2				0.83				0.77								0.59		
CHNO	Isocyanic acid	0.86		0.64	0.83		0.56		0.68			0.81			0.84	0.80	0.86		0.47
C4H6O4	succinic acid				0.83				0.71								0.60		
C6H6O3	trihydroxybenzene	0.83	0.48	0.72	0.82	0.85	0.62		0.79	0.42		0.75		0.71	0.59	0.82	0.54	0.59	0.49
C4H8O2	butyric acid				0.80				0.58								0.76		
C2H2NO3	C2H2NO3	0.61			0.79		0.48		0.56			0.49			0.63		0.90		
HO2H2O	HO2H2O	0.53			0.77				0.63								0.70		
CHN	Hydrogen cyanide	0.80		0.66	0.76	0.84	0.57	0.36	0.70			0.60		0.74	0.62	0.69	0.61	0.54	0.77
C6H6O2	Catechol	0.73			0.73		0.44		0.56						0.63		0.62		
C7H8O	Cresol	0.79			0.72		0.50		0.59						0.59		0.51		0.65
C3H4O4	Malonic acid				0.69				0.50								0.52	0.54	
C7H8O2	guaiacol	0.63			0.62	0.78			0.45	0.43				0.62	0.58		0.57		
C2H4O3	Glycolic Acid				0.62		0.42		0.63										
CNO	anion isocyanate	0.66		0.61	0.61		0.48		0.50			0.81			0.74	0.76	0.74		
C3H7NO2	L-Alanine				0.54				0.64										0.65
*NO		0.40			0.63				0.59								0.58		0.46
*NO2					0.45	0.51			0.41				0.50				0.54		
*Nox					0.60	0.47			0.57								0.59		
*CO		0.79	0.55		0.81	0.67	0.64		0.80	0.42				0.48	0.58		0.56		0.78
*SO2					0.63				0.57								0.52		0.72
ClNO3	Chlorine nitrate			0.45							0.45	0.69	0.53			0.66			
ClNO2	nitryl chloride			0.47								0.74	0.52			0.67			
Cl2	Chlorine												0.51						0.44
C6H5NO3	nitrophenol		0.41															0.55	

ALL = all dataset, LC = low concentrations, bfo = bonfire night, WL = winter-like.

The following paragraph has been added at the end of the section 4.3 OA factors and CIMS correlations, which supports the primary and secondary nature of PON:

during the bfo event, pPON_ME2 showed high r^2 values with carbon monoxide (0.78) as well as hydrogen cyanide (0.77), Methylformamide (0.65) and Dimethylformamide (0.63) which are typical primary pollutants related to combustion processes [(Borduas et al., 2015) and references therein]. sPON_ME2 showed low correlations with $ClNO_2$ (0.52) and $ClNO_3$ (0.53). High r^2 values were also observed during LC episode between $ClNO_2$ - $ClNO_3$ and LVOOA (0.67 - 0.66) and sPON (0.74 - 0.69) proving their secondary origin. Cl_2, which has been previously identified to be related to both primary and secondary sources (Faxon et al., 2015), shows low correlations with pPON_ME2 (0.44) during bfo event and sPON_ME2 (0.55) during LC event.

Minor Comments:

There are a large number of minor issues mostly about missing Tables, wrong numbering of Sections and typos in axis labels and such, so I only point out the two most obvious ones.

We are sorry for not updating the numbers and labelling in the last version of the manuscript before submitting it to ACPD. A full update of numbering to tables and figures has been performed.

- I mentioned that before, but all the references to other sections are wrong in the manuscript. Most importantly there are references to sections that don't even exist such as Section 3.4.1, in which supposedly the interference of m/z 30 is discussed. –

The interference of m/z 30 is being discussed in section 2.2.2

- Another glaring omission is Table 1 mentioned on page 9 line 325. This Table could be the most important evidence to support the separation of sPON from pPON, but is unfortunately missing.

This table is in supplement as Table S4.

References

Aiken, A. C., De Foy, B., Wiedinmyer, C., Decarlo, P. F., Ulbrich, I. M., Wehrli, M. N., Szidat, S., Prevot, A. S. H., Noda, J., Wacker, L., Volkamer, R., Fortner, E., Wang, J., Laskin, A., Shutthanandan, V., Zheng, J., Zhang, R., Paredes-Miranda, G., Arnott, W. P., Molina, L. T., Sosa, G., Querol, X., and Jimenez, J. L.: Mexico city aerosol analysis during milagro using high resolution aerosol mass spectrometry at the urban supersite (t0)-part 2: Analysis of the biomass burning contribution and the non-fossil carbon fraction, Atmos Chem Phys, 10, 5315-5341, 10.5194/acp-10-5315-2010, 2010.
Alfarra, M. R., Prevot, A. S. H., Szidat, S., Sandradewi, J., Weimer, S., Lanz, V. A., Schreiber, D., Mohr, M., and Baltensperger, U.: Identification of the mass spectral signature of organic aerosols from wood burning emissions, Environmental Science & Technology, 41, 5770-5777, Doi 10.1021/Es062289b, 2007.
Allan, J. D., Delia, A. E., Coe, H., Bower, K. N., Alfarra, M. R., Jimenez, J. L., Middlebrook, A. M., Drewnick, F., Onasch, T. B., Canagaratna, M. R., Jayne, J. T., and Worsnop, D. R.: A generalised method for the extraction of chemically resolved mass spectra from aerodyne aerosol mass spectrometer data, J Aerosol Sci, 35, 909-922, DOI 10.1016/j.jaerosci.2004.02.007, 2004.
Allan, J. D., Alfarra, M. R., Bower, K. N., Coe, H., Jayne, J. T., Worsnop, D. R., Aalto, P. P., Kulmala, M., Hyötyläinen, T., Cavalli, F., and Laaksonen, A.: Size and composition measurements of background aerosol and new particle growth in a finnish forest during quest 2 using an aerodyne aerosol mass spectrometer, Atmos. Chem. Phys., 6, 315-327, 10.5194/acp-6-315-2006, 2006.
Allan, J. D., Williams, P. I., Morgan, W. T., Martin, C. L., Flynn, M. J., Lee, J., Nemitz, E., Phillips, G. J., Gallagher, M. W., and Coe, H.: Contributions from transport, solid fuel burning and cooking to primary organic aerosols in two uk cities, Atmos Chem Phys, 10, 647-668, 2010.
Borduas, N., da Silva, G., Murphy, J. G., and Abbatt, J. P. D.: Experimental and theoretical understanding of the gas phase oxidation of atmospheric amides with oh radicals: Kinetics, products, and mechanisms, The Journal of Physical Chemistry A, 119, 4298-4308, 10.1021/jp503759f, 2015.
Bruns, E. A., Krapf, M., Orasche, J., Huang, Y., Zimmermann, R., Drinovec, L., Močnik, G., El-Haddad, I., Slowik, J. G., Dommen, J., Baltensperger, U., and Prévôt, A. S. H.: Characterization of primary and secondary wood combustion products generated under different burner loads, Atmos. Chem. Phys., 15, 2825-2841, 10.5194/acp-15-2825-2015, 2015.
Canagaratna, M. R., Jayne, J. T., Ghertner, D. A., Herndon, S., Shi, Q., Jimenez, J. L., Silva, P. J., Williams, P., Lanni, T., Drewnick, F., Demerjian, K. L., Kolb, C. E., and Worsnop, D. R.: Chase studies of particulate emissions from in-use new york city vehicles, Aerosol Science and Technology, 38, 555-573, 10.1080/02786820490465504, 2004.

Chakraborty, A., Gupta, T., and Tripathi, S. N.: Chemical composition and characteristics of ambient aerosols and rainwater residues during indian summer monsoon: Insight from aerosol mass spectrometry, Atmos Environ, 136, 144-155, 10.1016/j.atmosenv.2016.04.024, 2016.
Collier, S., Zhou, S., Onasch, T. B., Jaffe, D. A., Kleinman, L., Sedlacek, A. J., Briggs, N. L., Hee, J., Fortner, E., Shilling, J. E., Worsnop, D., Yokelson, R. J., Parworth, C., Ge, X., Xu, J., Butterfield, Z., Chand, D., Dubey, M. K., Pekour, M. S., Springston, S., and Zhang, Q.: Regional influence of aerosol emissions from wildfires driven by combustion efficiency: Insights from the bbop campaign, Environmental Science & Technology, 50, 8613-8622, 10.1021/acs.est.6b01617, 2016.
Corbin, J. C., Keller, A., Lohmann, U., Burtscher, H., Sierau, B., and Mensah, A. A.: Organic emissions from a wood stove and a pellet stove before and after simulated atmospheric aging, Aerosol Science and Technology, 49, 1037-1050, 10.1080/02786826.2015.1079586, 2015a.
Corbin, J. C., Lohmann, U., Sierau, B., Keller, A., Burtscher, H., and Mensah, A. A.: Black carbon surface oxidation and organic composition of beech-wood soot aerosols, Atmos. Chem. Phys., 15, 11885-11907, 10.5194/acp-15-11885-2015, 2015b.
Drewnick, F., Diesch, J. M., Faber, P., and Borrmann, S.: Aerosol mass spectrometry: Particle–vaporizer interactions and their consequences for the measurements, Atmos. Meas. Tech., 8, 3811-3830, 10.5194/amt-8-3811-2015, 2015.
Elser, M., Huang, R. J., Wolf, R., Slowik, J. G., Wang, Q., Canonaco, F., Li, G., Bozzetti, C., Daellenbach, K. R., Huang, Y., Zhang, R., Li, Z., Cao, J., Baltensperger, U., El-Haddad, I., and André, P.: New insights into pm2.5 chemical composition and sources in two major cities in china during extreme haze events using aerosol mass spectrometry, Atmos Chem Phys, 16, 3207-3225, 10.5194/acp-16-3207-2016, 2016.
Farmer, D. K., Matsunaga, A., Docherty, K. S., Surratt, J. D., Seinfeld, J. H., Ziemann, P. J., and Jimenez, J. L.: Response of an aerosol mass spectrometer to organonitrates and organosulfates and implications for atmospheric chemistry, Proceedings of the National Academy of Sciences of the United States of America, 107, 6670-6675, 10.1073/pnas.0912340107, 2010.
Faxon, C., Bean, J., and Ruiz, L.: Inland concentrations of cl2 and clno2 in southeast texas suggest chlorine chemistry significantly contributes to atmospheric reactivity, Atmosphere, 6, 1487, 2015.
Florou, K., Papanastasiou, D. K., Pikridas, M., Kaltsonoudis, C., Louvaris, E., Gkatzelis, G. I., Patoulias, D., Mihalopoulos, N., and Pandis, S. N.: The contribution of wood burning and other pollution sources to wintertime organic aerosol levels in two greek cities, Atmos. Chem. Phys., 17, 3145-3163, 10.5194/acp-17-3145-2017, 2017.
Hao, L. Q., Kortelainen, A., Romakkaniemi, S., Portin, H., Jaatinen, A., Leskinen, A., Komppula, M., Miettinen, P., Sueper, D., Pajunoja, A., Smith, J. N., Lehtinen, K. E. J., Worsnop, D. R., Laaksonen, A., and Virtanen, A.: Atmospheric submicron aerosol composition and particulate organic nitrate formation in a boreal forestland-urban mixed region, Atmos Chem Phys, 14, 13483-13495, 10.5194/acp-14-13483-2014, 2014.
He, L. Y., Lin, Y., Huang, X. F., Guo, S., Xue, L., Su, Q., Hu, M., Luan, S. J., and Zhang, Y. H.: Characterization of high-resolution aerosol mass spectra of primary organic aerosol emissions from chinese cooking and biomass burning, Atmos. Chem. Phys., 10, 11535-11543, 10.5194/acp-10-11535-2010, 2010.
Heringa, M. F., DeCarlo, P. F., Chirico, R., Tritscher, T., Dommen, J., Weingartner, E., Richter, R., Wehrle, G., Prévôt, A. S. H., and Baltensperger, U.: Investigations of primary and secondary particulate matter of different wood combustion appliances with a high-resolution time-of-flight aerosol mass spectrometer, Atmos. Chem. Phys., 11, 5945-5957, 10.5194/acp-11-5945-2011, 2011.
Kiendler-Scharr, A., Mensah, A. A., Friese, E., Topping, D., Nemitz, E., Prevot, A. S. H., Äijälä, M., Allan, J., Canonaco, F., Canagaratna, M., Carbone, S., Crippa, M., Dall Osto, M., Day, D. A., De Carlo, P., Di Marco, C. F., Elbern, H., Eriksson, A., Freney, E., Hao, L., Herrmann, H., Hildebrandt, L., Hillamo, R., Jimenez, J. L., Laaksonen, A., McFiggans, G., Mohr, C., O'Dowd, C., Otjes, R., Ovadnevaite, J., Pandis, S. N., Poulain, L., Schlag, P., Sellegri, K., Swietlicki, E., Tiitta, P., Vermeulen, A., Wahner, A.,

Worsnop, D., and Wu, H. C.: Ubiquity of organic nitrates from nighttime chemistry in the european submicron aerosol, Geophys Res Lett, 43, 7735-7744, 10.1002/2016gl069239, 2016.
Kostenidou, E., Florou, K., Kaltsonoudis, C., Tsiflikiotou, M., Vratolis, S., Eleftheriadis, K., and Pandis, S. N.: Sources and chemical characterization of organic aerosol during the summer in the eastern mediterranean, Atmos. Chem. Phys., 15, 11355-11371, 10.5194/acp-15-11355-2015, 2015.
Mohr, C., DeCarlo, P. F., Heringa, M. F., Chirico, R., Slowik, J. G., Richter, R., Reche, C., Alastuey, A., Querol, X., Seco, R., Penuelas, J., Jimenez, J. L., Crippa, M., Zimmermann, R., Baltensperger, U., and Prevot, A. S. H.: Identification and quantification of organic aerosol from cooking and other sources in barcelona using aerosol mass spectrometer data, Atmos Chem Phys, 12, 1649-1665, DOI 10.5194/acp-12-1649-2012, 2012.
Ng, N. L., Canagaratna, M. R., Zhang, Q., Jimenez, J. L., Tian, J., Ulbrich, I. M., Kroll, J. H., Docherty, K. S., Chhabra, P. S., Bahreini, R., Murphy, S. M., Seinfeld, J. H., Hildebrandt, L., Donahue, N. M., DeCarlo, P. F., Lanz, V. A., Prevot, A. S. H., Dinar, E., Rudich, Y., and Worsnop, D. R.: Organic aerosol components observed in northern hemispheric datasets from aerosol mass spectrometry, Atmos Chem Phys, 10, 4625-4641, DOI 10.5194/acp-10-4625-2010, 2010.
Ortega, A. M., Day, D. A., Cubison, M. J., Brune, W. H., Bon, D., de Gouw, J. A., and Jimenez, J. L.: Secondary organic aerosol formation and primary organic aerosol oxidation from biomass-burning smoke in a flow reactor during flame-3, Atmos. Chem. Phys., 13, 11551-11571, 10.5194/acp-13-11551-2013, 2013.
Reyes-Villegas, E., Green, D. C., Priestman, M., Canonaco, F., Coe, H., Prévôt, A. S. H., and Allan, J. D.: Organic aerosol source apportionment in london 2013 with me-2: Exploring the solution space with annual and seasonal analysis, Atmos. Chem. Phys., 16, 15545-15559, 10.5194/acp-16-15545-2016, 2016.
Slowik, J. G., Vlasenko, A., McGuire, M., Evans, G. J., and Abbatt, J. P.: Simultaneous factor analysis of organic particle and gas mass spectra: Ams and ptr-ms measurements at an urban site, Atmos Chem Phys, 10, 1969-1988, 2010.
Sun, Y. L., Zhang, Q., Schwab, J. J., Yang, T., Ng, N. L., and Demerjian, K. L.: Factor analysis of combined organic and inorganic aerosol mass spectra from high resolution aerosol mass spectrometer measurements, Atmos Chem Phys, 12, 8537-8551, DOI 10.5194/acp-12-8537-2012, 2012.
Tiitta, P., Leskinen, A., Hao, L., Yli-Pirilä, P., Kortelainen, M., Grigonyte, J., Tissari, J., Lamberg, H., Hartikainen, A., Kuuspalo, K., Kortelainen, A. M., Virtanen, A., Lehtinen, K. E. J., Komppula, M., Pieber, S., Prévôt, A. S. H., Onasch, T. B., Worsnop, D. R., Czech, H., Zimmermann, R., Jokiniemi, J., and Sippula, O.: Transformation of logwood combustion emissions in a smog chamber: Formation of secondary organic aerosol and changes in the primary organic aerosol upon daytime and nighttime aging, Atmos. Chem. Phys., 16, 13251-13269, 10.5194/acp-16-13251-2016, 2016.
Xu, L., Suresh, S., Guo, H., Weber, R. J., and Ng, N. L.: Aerosol characterization over the southeastern united states using high-resolution aerosol mass spectrometry: Spatial and seasonal variation of aerosol composition and sources with a focus on organic nitrates, Atmos. Chem. Phys., 15, 7307-7336, 10.5194/acp-15-7307-2015, 2015.
Zhang, J. K., Cheng, M. T., Ji, D. S., Liu, Z. R., Hu, B., Sun, Y., and Wang, Y. S.: Characterization of submicron particles during biomass burning and coal combustion periods in beijing, china, Science of The Total Environment, 562, 812-821, 10.1016/j.scitotenv.2016.04.015, 2016.
Zhou, S., Collier, S., Jaffe, D. A., Briggs, N. L., Hee, J., Sedlacek Iii, A. J., Kleinman, L., Onasch, T. B., and Zhang, Q.: Regional influence of wildfires on aerosol chemistry in the western us and insights into atmospheric aging of biomass burning organic aerosol, Atmos. Chem. Phys., 17, 2477-2493, 10.5194/acp-17-2477-2017, 2017.
Zhu, Q., He, L. Y., Huang, X. F., Cao, L. M., Gong, Z. H., Wang, C., Zhuang, X., and Hu, M.: Atmospheric aerosol compositions and sources at two national background sites in northern and southern china, Atmos. Chem. Phys., 16, 10283-10297, 10.5194/acp-16-10283-2016, 2016.

Simultaneous Aerosol Mass Spectrometry and Chemical Ionisation Mass Spectrometry measurements during a biomass burning event in the UK: Insights into nitrate chemistry

Ernesto Reyes-Villegas[1], Michael Priestley[1], Yu-Chieh Ting[1], Sophie Haslett[1], Thomas Bannan[1], Michael Le breton[1*], Paul I. Williams[1,2], Asan Bacak[1], Michael J. Flynn[1], Hugh Coe[1], Carl Percival[1Δ], James D. Allan[1,2]

[1]School of Earth, Atmospheric and Environmental Sciences, The University of Manchester, Manchester, M13 9PL, UK
[2]National Centre for Atmospheric Science, The University of Manchester, Manchester, M13 9PL, UK
[*]Now at University of Gothenburg, 40530 Gothenburg, Sweden
[Δ]Now at Jet Propulsion Laboratory, 4800 Oak Grove Drive, Pasadena, CA 91109, USA

Correspondence to: Ernesto Reyes-Villegas (ernesto.reyesvillegas@manchester.ac.uk)

Abstract. Over the past decade, there has been an increasing interest in short-term events that negatively affect air quality such as bonfires and fireworks. High aerosol and gas concentrations generated from public bonfires/fireworks were measured in order to understand the night-time chemical processes and their atmospheric implications. Nitrogen chemistry was observed during the bonfire night with nitrogen containing compounds in both gas and aerosol phase and further N_2O_5 and $ClNO_2$ concentrations, which depleted early next morning due to photolysis of NO_3 radicals, ceasing production. Particulate organic oxides of nitrogen (PON) concentrations of 2.8 µg.m^{-3} were estimated using the m/z 46:30 ratios from AMS measurements, according to previously published methods. ME-2 source apportionment was performed to determine organic aerosol concentrations from different sources after modifying the fragmentation table and it was possible to identify two PON factors representing primary (pPON_ME2) and secondary (sPON_ME2) contributions. A slight improvement in the agreement between the source apportionment of the AMS and a collocated AE-31 Aethalometer was observed after modifying the prescribed fragmentation in the AMS organic spectrum (the fragmentation table) to determine PON sources, which resulted in an r^2 = 0.894 between BBOA and b_{abs_470wb} compared to an r^2 = 0.861 obtained without the modification. Correlations between OA sources and measurements made using Time of Flight Chemical Ionization Mass Spectrometry with an iodide adduct ion were performed in order to determine possible gas tracers to be used in future ME-2 analyses to constrain solutions. During bonfire night, high correlations (r^2) were observed between BBOA and methacrylic acid (0.92), Acrylic acid (0.90), nitrous acid (0.86), propionic acid, (0.85) and Hydrogen cyanide (0.76). A series of oxygenated species, chlorine compounds showed good correlations with sPON_ME2 and the low volatility oxygenated organic aerosol (LVOOA) factor during bonfire night and an event with low pollutant concentrations. Further analysis of pPON_ME2 and sPON_ME2 was performed in order to determine whether these PON sources absorb light near the UV region using an Aethalometer. This hypothesis was tested by doing multilinear regressions between b_{abs_470wb} and BBOA, sPON_ME2 and pPON_ME2. Our results suggest that sPON_ME2 does not absorb light at 470 nm while pPON_ME2 and LVOOA absorb light at 470 nm. This may inform black carbon (BC) source apportionment studies from Aethalometer measurements, through investigation of the brown carbon contribution to b_{abs_470wb}.

Comment [ERV1]: Paragraph edited in response to comment 2 (3) of Referee 1.

1. Introduction.

Exposure to combustion aerosols has been associated with a range of negative health effects, in particular wood smoke aerosols have been shown to present respiratory and cardiovascular health effects (Naeher et al., 2007). Bonfires and fireworks are one of the main sporadic events with high emissions of atmospheric pollutants (Vassura et al., 2014;Joshi et al., 2016), even when these high emissions only last a couple of hours, high pollutant concentrations may instigate adverse

effects on human health (Moreno et al., 2007;Godri et al., 2010) and severely reduce visibility (Vecchi et al., 2008). Ravindra et al. (2003) found that the short-term exposure of air pollutants increases the likelihood of acute health effects.

Due to these adverse effects, different studies have been performed to analyse air pollution during important festivities around the world, for instance New Year's Eve celebrations (Drewnick et al., 2006;Zhang et al., 2010), the Lantern Festival in China (Wang et al., 2007) and Diwali festival in India (Pervez et al., 2016) as well as football matches such as during the Bundesliga in Mainz Germany 2012 (Faber et al., 2013). In the UK, the bonfire night festivity takes place on November 5th to commemorate Guy Fawkes' unsuccessful attempt to destroy the Houses of Parliament in 1605 (Ainsworth, 1850). During this celebration, bonfires usually followed by fireworks, are lit domestically and on larger scale communally in public parks. Different studies have been carried out to assess the air pollution during bonfire night in the UK; for instance targeting the particle size distribution (Colbeck and Chung, 1996), investigating PM_{10} concentrations in different cities around the UK during bonfires (Clark, 1997), measuring dioxins in ambient air in Oxford (Dyke et al., 1997); polycyclic aromatic hydrocarbons were measured in Lancaster, 2000 (Farrar et al., 2004) and potentially toxic elements were measured and their association to health risks was assessed in London (Hamad et al., 2015).

Receptor modelling has been widely used to determine OA sources in urban environments. However, it has been used in just a small number of studies with sporadic events of high pollutant concentrations. For instance Vecchi et al. (2008) was the first to analyse measurements taken during firework displays using positive matrix factorisation (PMF). Tian et al. (2014) did a PMF analysis of $PM_{2.5}$ components, identifying five different sources: Crustal dust, coal combustion, secondary particles, vehicular exhaust and fireworks. In Riccione, Italy, Vassura et al. (2014) determined that levoglucosan, OC, PAHs, Al, and Pb, emitted from bonfires during St. Joseph's Eve, can be used as markers for bonfire emissions.

Particulate organic oxides of nitrogen (PON), a term we use here to encompass nitro-organics and organic nitrates, have been found to absorb light near the UV region (Mohr et al., 2013) and to present potential toxicity affecting human health (Fernandez et al., 1992;Qingguo et al., 1995). PON also act as a NO_x reservoir in the night-time, releasing NO_x concentrations when the sun rises with the possibility of increasing O_3 production (Perring et al., 2013;Mao et al., 2013). PON are important components of organic aerosols; for instance Day et al. (2010), in measurements taken during winter at an urban location, found that PON concentrations accounted for up to 10% of organic matter. Kiendler-Scharr et al. (2016) concluded that, at a continental scale, PON represent 34% to 44% of aerosol nitrate. Organic oxides of nitrogen can be categorised, according to their origin, into two types; primary and secondary, primary organic nitrates are related to combustion sources (Zhang et al., 2016) such as fossil fuel (Day et al., 2010) and biomass burning emissions (Kitanovski et al., 2012;Mohr et al., 2013). Secondary organic oxides of nitrogen are produced in the atmosphere, for example when NO_3 reacts with unsaturated hydrocarbons (Ng et al., 2017). Nitrophenols are produced from reactions of phenols, both during the day reacting with OH + NO_2, and at night reacting with NO_3 +NO_2 (Harrison et al., 2005;Yuan et al., 2016).

Comment [ERV2]: Citation edited. Minor coment 1 Referee 1.

The Aethalometer (Magee Scientific, USA) has been widely used to measure light absorbing carbon, proving to be a robust instrument capable to operate in a variety of environments and currently is being used at many different locations around the world. The European Environment Agency, in a technical report published in 2013 (EEA, 2013), states that there are at least 11 European countries using Aethalometers. The UK has a black carbon (BC) network comprising 14 sites covering a wide range of monitoring sites (https://uk-air.defra.gov.uk/networks/network-info?view=ukbsn) and India started in 2016 a BC network with 16 Aethalometers (LASKAR et al., 2016). Commonly, Aethalometers have been used to separate sources of light-absorbing aerosols following Sandradewi et al. (2008). The approach separates absorption from traffic, predominately resulting from BC which absorbs light in the infrared region and from wood burning, which includes BC and absorbing organic matter that also absorbs near the ultraviolet region. The Aethalometer model is based in the differences of aerosol absorption, using the absorption Ångström exponent, at specific wavelength of light chosen to perform the model.

Absorption Ångström exponent values range from 0.8-1.1 for traffic and 0.9-3.5 for wood burning (Zotter et al., 2017). It is known that Brown carbon (BrC) is organic matter capable of absorbing light near the UV region (Bones et al., 2010;Saleh et al., 2014) and that PON is a potential contributor to BrC (Mohr et al., 2013). However, the mechanistic behaviour that links this behaviour to wood burning has not completely been resolved and there may be other sources such as secondary organic aerosols that can absorb near the UV region.

Here we present analysis performed on data collected during bonfire night celebrations in Manchester UK (29th October to 10th November 2014) using a cToF-AMS and a HR-ToF-CIMS along with other instruments to measure both aerosols and gaseous pollutants with the aim of understanding the night-time chemical processes and their atmospheric implications. Very high concentrations of pollutants occurred as a result of the meteorological conditions, which presented a good opportunity to investigate the detailed phenomenon as a case study, particularly the possibility to determine PON concentrations, their nature and interaction with Aethalometer measurements.

2. Methods

2.1 Site and instrumentation

Online measurements of aerosols and gases were taken from ambient air, between 29th October and 10th November 2014, at a rooftop location at the University of Manchester [53.467° N, 2.232° W], in order to quantify atmospheric pollution during the bonfire night event on and around 5th November. Figure S1 shows a map with the location of the monitoring site and nine public parks where bonfire/fireworks were displayed around greater Manchester. This is the same dataset presented by Liu et al. (2017).

A compact time of flight Aerosol Mass Spectrometer (cToF-AMS, here after AMS) was used to perform 5-minute measurements of organic aerosols (OA), sulfate (SO_4^{2-}), nitrate (NO_3^-), ammonium ($NH4^+$) and chloride (Cl^-) (Drewnick et al., 2005). This version of AMS provides unit mass resolution mass spectra information. A High Resolution Time of Flight Chemical Ionization Mass Spectrometer (HR-ToF-CIMS, here after CIMS) was used to measure gas phase concentrations, using iodide as a reagent (Lee et al., 2014). The methodology to calculate gas phase concentrations from CIMS measurements are been described by Priestley et al. (In preparation). An Aethalometer, model AE31 (Magee Scientific), measured light absorption at seven wavelengths (370, 450, 571, 615, 660, 880 and 950 nm) and a Multi Angle Absorption Photometer (MAAP; Thermo Model 5012) measured BC concentrations (Petzold et al., 2002). NO_x, CO, O_3 and meteorology data were downloaded from Whitworth observatory (http://www.cas.manchester.ac.uk/restools/whitworth/data/), which were measured at the same location. From 31st October to 10th November, a catalytic stripper was attached to the AMS, switching every 30 minutes between direct measurements and through the catalytic stripper. These measurements were performed as part of a different experiment (Liu et al., 2017). In the present study we used the AMS data from the direct measurements only, aerosol and gas data from other instruments were averaged to AMS sampling times.

2.2 Source apportionment

2.2.1 Aethalometer model

The aerosol light absorption depends on the wavelength and may be used to apportion BC from traffic and wood burning from Aethalometer measurements as proposed by (Sandradewi et al., 2008). The absorption coefficients (b_{abs}) are related to the wavelengths at which the absorptions are measured (λ) and Ångström absorption exponents (α) with the relationship: $b_{abs} \propto \lambda^{\alpha i}$, thus the following equations can be solved:

$$\frac{b_{abs\_470tr}}{b_{abs\_950tr}} = \left(\frac{470}{950}\right)^{-\alpha_{tr}} \quad (1)$$

$$\frac{b_{abs\_470wb}}{b_{abs\_950wb}} = \left(\frac{470}{950}\right)^{-\alpha_{wb}} \quad (2)$$

$$b_{abs}(470_{nm}) = b_{abs\_470tr} + b_{abs\_470wb} \quad (3)$$

$$b_{abs}(950_{nm}) = b_{abs\_950tr} + b_{abs\_950wb} \quad (4)$$

Here, it is possible to calculate the wood burning (wb) and traffic (tr) contributions to BC at 470 and 950 nanometres (nm) as used in previous studies (Crilley et al., 2015;Harrison et al., 2012). Wavelengths 470 and 950 nm were chosen as Zotter et al. (2017) determined that using this pair of wavelength resulted in less residuals compared when using the pair of wavelengths 470-880, and 370-880 nm. Before the Aethalometer model was applied, the absorption coefficients (b_{abs}) needed to be corrected following Weingartner et al. (2003) as attenuation is affected by scattering and loading variations. The following parameters were calculated: multiple scattering constant C = 3.16 and filter loading factors (f) of 1.49 and 1.28 for the wavelengths 470 and 950 nm respectively. Refer to section S3 in supplement for detailed information.

2.2.2 Particulate Organic Oxides of Nitrogen (PON)

Concentrations of PON were calculated following the method proposed by Farmer et al. (2010) and the considerations used by Kiendler-Scharr et al. (2016). This method has been previously used in studies looking at aerosols from biomass burning (Tiitta et al., 2016;Zhu et al., 2016;Florou et al., 2017). Equation 5 calculates the PON fraction (X_{PON}), using the signals at m/z 30 and m/z 46 to calculate m/z ratios 46:30 from AMS measurements (R_{meas}), from ammonium nitrate calibrations (R_{cal}), and from organic nitrogen (R_{ON}) to quantify PON concentrations.

$$X_{PON} = \frac{(R_{meas} - R_{Cal})(1+R_{ON})}{(R_{ON} - R_{cal})(1+R_{meas})} \quad (5)$$

Where ratios from ammonium nitrate calibrations R_{cal} = 0.5; R_{meas} = m/z 46:30 ratio from measurements; m/z 46:30 ratio from ON R_{ON} = 0.1, Following Kostenidou et al. (2015) consideration, R_{ON} = 0.1 was calculated as the minimum m/z 46:30 ratio observed. R_{ON} value of 0.1 has been used in previous studies (Kiendler-Scharr et al., 2016;Tiitta et al., 2016).

$$PON = X_{PON} * NO_3^- \quad (6)$$

Finally, equation 6 calculates PON concentrations [µg.m^{-3}] where NO_3^- is the total nitrate measured by the cToF-AMS. The method proposed by Farmer et al. (2010) is based on HR-ToF-AMS measurements were m/z 30 represents NO^+ ion and m/z 46 NO_2^+ ion while the cToF-AMS gives unit mass resolution mass spectra information, hence, there is the possibility to have interference of CH_2O^+ ion at m/z 30. However, when analysing mass spectra from previous laboratory and ambient studies using HR-ToF-AMS to investigate biomass burning emissions, we can confirm that the signal of CH_2O^+ at m/z 30 is low compared to signals at m/z's 29 and 31, while in this study m/z 30 is the main signal (Fig. 5.c). Hence, in this study an interference of CH_2O^+ at m/z 30 is unlikely and if there were any interference of CH_2O^+ it would be negligible. Table S1 in supplement shows m/z 30/29 and 30/31 from previous laboratory and ambient studies investigating biomass burning emissions.

Another possible interference would be the presence of mineral nitrates at m/z 30 (e.g. KNO_3 and $NaNO_3$). However, mineral nitrate salts tend to be large particles (Allan et al., 2006;Chakraborty et al., 2016) and also have low vaporisation efficiency (Drewnick et al., 2015), which makes it unlikely to be measured by the AMS in large quantities.

Comment [ERV3]: This section has been added to methodology in response to minor comment 2 Referee 1 and major comment of Referee 2 about quantification of PON from biomass burning using a cToF-AMS

Comment [ERV4]: Table S1 in supplement gives detailed information about possible CH2O+ interference. Responding major comment of Referee 2 about quantification of PON from biomass burning using a cToF-AMS

2.2.3 Multilinear engine 2 (ME-2)

Multilinear engine 2 (Paatero, 1999) is a multivariate solver used to determine factors governing the behaviour of a two dimensional data matrix, which then can be interpreted as pollutant sources. ME-2 uses the same data model as positive matrix factorisation, which is also a receptor model that performs factorisation by using a weighted least squares approach (Paatero and Tapper, 1994).

In order to explore the solution space, ME-2 is capable of using information from previous studies, for example pollutant time series or mass spectra, as inputs to the model (named target time series and target profiles respectively) to constrain the runs. These constraints are performed using the a-value approach, to determine the extent to which the output is allowed to vary. For example, by using an a-value of 0.1 to a specific source, the user is allowing the output to vary 10% from the input. For more details refer to Canonaco et al. (2013).

In this study, ME-2 and PMF were used through the source finder interface, SoFi version 4.8 (Canonaco et al., 2013) to identify OA sources using the suggestions made by Crippa et al. (2014) and the strategy proposed by Reyes-Villegas et al. (2016). ME-2 was performed using mass spectra (BBOA, HOA and COA) from two different studies as target profiles (TP) to constrain the runs; London (Young et al., 2015) and Paris (Crippa et al., 2013), Figure S5 explains the labelling used to identify the different runs.

Solutions were explored with PMF using different fpeak values (ranging from -1.0 to 1.0 with steps of 0.1) and ME-2 using different a-values, (nine runs with London TP and nine runs with Paris TP), looking at four, five and six-factor solutions. Section S7.1 shows the strategy used to determine the optimal solution. Factorisation struggles to separate two or more sources if they are highly correlated, for example during stagnant conditions due to low temperatures and wind speed, which was the case during the bonfire night 2014. The pollutants were well-mixed, making it difficult to separate the sources. Hence, four tests were performed using different time sets in order to identify the best way to perform source apportionment:

- Test 1 performs factorisation on all the dataset.
- Test 2 involves factorising the event before and after bonfire night and using mass spectra from this analysis as TP to factorise the bonfire night event.
- Test 3 involves factorising the bonfire night event and using mass spectra from this analysis as TP as applied to the complete dataset.
- Test 4 involves factorising the event before and after bonfire night and using mass spectra from this analysis as TP to factorise the full dataset.

PON may exhibit covariance with other types of OA, thus their inclusion in the source apportionment analysis may give a more complete factorisation and highlight their co-emission with other OA types. Previous studies have quantified PON concentrations from AMS-PMF analysis to both rural and urban measurements (Sun et al., 2012;Hao et al., 2014;Xu et al., 2015;Zhang et al., 2016). In this study, an experiment was designed by modifying the fragmentation table, through the AMS analysis toolkit 1.56, in order to identify a PON source. The fragmentation table contains the different chemical species measured by the AMS, with each row representing m/z for specific species and where the user can define peaks that exist in each species' partial mass spectrum and their dependency on other peaks (Allan et al., 2004). The following steps were performed to modify the fragmentation table:

- Time series of a new ratio named R_{ON_30} is calculated by R_{ON_30} = PON/mz30, were PON is the time series calculated in section 2.2.2 and mz30 is the time series of the signal at m/z=30 measured by the AMS.

Comment [ERV5]: Paragraph edited in response to comment 3 (3) of Referee 1.

- Using the AMS analysis toolkit; the fragmentation table is modified, in the column frag_Organic at the m/z 30, by multiplying R_{ON_30}*30. See figure S4 in supplement for a screenshot of the fragmentation table.

- PMF inputs are generated to be used in SoFi software.

Comment [ERV6]: The explanation of the fragmentation table has been edited and a screenshot of the fragmentation table has been added to supplement (Figure S4) for a better explanation. Paragraph edited in response to comment of Referee 2 related to the fragmentation table.

3. Results

3.1 Meteorology and pollutant overview

During bonfire night festivities on November 5th, a temperature of 4 ˚C and wind speed of 1.5 $m.s^{-1}$ were observed (Fig. 1.a), causing stagnant conditions which facilitated pollutant accumulation. Looking at the time series for the whole sampling time (Fig. 1.b), it was possible to observe four separate events with different pollutant behaviour (marked with coloured lines over the x-axis in Fig. 1), driven by different meteorological conditions: one event had high secondary concentrations (HSC, yellow line) from October 30th to November 1st, which experienced a relatively high temperature of 17-20 ˚C; one event of low pollutant concentrations (LC, grey line) from November 1st - 3rd was observed when continental air masses were present; Bonfire night (bfo, blue line), with a temperature of 4 ˚C; and a winter-like episode (WL, purple line) from November 8th - 10th, with temperatures of 5-6 ˚C and high primary pollutant concentrations. Figure S3 in supplement shows backtrajectories of the different events.

Aerosol concentrations during bonfire night were particularly high (Fig. 1.c), with the highest peak concentrations of 65.0, 19.0, 6.8, 6.0, 5.9 and 3.2 $\mu g.m^{-3}$ for OA, BC, SO_4, Cl, NH_4 and NO_3 respectively measured around 20:30 hrs on November 5th. It is worth noting how high these concentrations are compared to concentrations before and after bonfire night (Fig. 1.b) where aerosol concentrations ranged from 0.5 – 7.0 $\mu g.m^{-3}$. Measured PM_1 concentrations (sum of BC, organic and inorganic aerosols) of 115 $\mu g.m^{-3}$ (Fig. 1.c) were observed during bonfire night.

Looking at the daily concentrations (Fig. 1.d), it is possible to observe PM_1 daily concentrations of 25 $\mu g.m^{-3}$ on bonfire night compared to the low concentrations observed between November 1st – 2nd with concentrations ranging between 3-4 $\mu g.m^{-3}$. The impact of the emissions during bonfire night is present even during the next day with PM_1 concentrations of 14 $\mu g.m^{-3}$.

Gas phase pollutants were measured at the Whitworth observatory. Figure 2 shows high SO_2, CO and NO_x concentrations during bonfire night; these primary pollutants are well known to be combustion related pollutants. The high SO_2 concentrations during bonfire night are expected as solid fuels such as wood emit SO_2 when burned. This can also explain the SO_2 peak in the night of November 10th - 11th when SO_2 concentrations may be related to solid fuels used for domestic heating as a result of the low temperatures (6 ˚C). CO and NO were present at higher concentrations during bonfire night compared to previous days with concentrations reaching 1600 ppb (CO) 99 ppb (NO) during bonfire night compared to November 1st with concentrations of 230 ppb of CO and 16 ppb of NO. Some O_3 concentrations were measured during bonfire night, but given the very high NO concentrations, these are considered to be an interference with the measurement.

3.2 Bonfire night analysis

3.2.1 Traffic and wood burning contributions to BC

OA concentrations started increasing at 19:30 hrs while BC concentrations started increasing two hours earlier around 17:00 hrs (Fig. 1.c). This rise in BC concentrations may be due to bonfire emissions, although they may also be related to traffic emissions; thus the Aethalometer model was used to identify both traffic and wood burning contributions to BC.

Once, b_{abs} are corrected, equations shown in section 2.2.1 are used to apply the Aethalometer model, with Ångström absorption exponents (α) of 1.0 for traffic (α_{tr}), using the wavelength 470 nm, and 2.0 for wood burning (α_{wb}) using the wavelength 950 nm, to determine traffic and wood burning contributions. Figure 3 shows the absorption coefficients for wood burning b_{abs_470wb} (blue) and traffic b_{abs_950tr} (red), both increasing around 17:00-18:00 hrs to values lower than 100 Mm^{-1} while b_{abs}, indicating contributions from wood burning and traffic during this event. It is when the majority of bonfire events are taking place, around 20:00, when b_{abs_470wb} shows the greatest increase, with values reaching 480 Mm^{-1} compared to 150 Mm^{-1} for b_{abs_950tr}.

3.2.2 PON identification and quantification

Currently, there is not a direct technique to quantify on-line integrated PON concentrations. However, it is possible to estimate PON concentrations from AMS measurements using the m/z 46:30 ratios (Farmer et al., 2010) as explained in section 2.2.2. This event during bonfire night 2014, with high pollutant concentrations, provided the opportunity to identify the presence of PON. Inorganic nitrate from NH_4NO_3 has been detected at m/z 46:30 ratios between 0.33 and 0.5 (Alfarra et al., 2006) and of 0.37 (Fry et al., 2009), although each instrument-specific ratio is determined during routine calibrations. PON has been identified with m/z 46:30 ratios of 0.07-0.10 (Hao et al., 2014) and 0.17-0.26 (Sato et al., 2010). In this study, m/z 46:30 ratios of 0.11-0.18 were observed during bonfire night (Fig. 4), confirming the presence of PON during this event. Figure 4 shows PON concentrations of up to 2.8 $\mu g.m^{-3}$ during bonfire night, which are over the detection limit of 0.1 $\mu g.m^{-3}$ reported by Bruns et al. (2010). PON concentrations are considered high compared to previous studies with concentrations between 0.03 – 1.2 $\mu g.m^{-3}$, from a wide variety of sites across Europe (Kiendler-Scharr et al., 2016), while high PON concentrations of 4.2 $\mu g.m^{-3}$ were observed during a biomass burning event in Beijing, China (Zhang et al., 2016).

3.3 OA source apportionment

Comment [ERV7]: Following comments of both Referees, only the optimal solutions (test2_ON) is explained in the main and solution test2 has been moved to appendix A

This event with high pollutant concentrations during bonfire night gave the opportunity to test ME-2 factorisation tool under these conditions and determine the best way to perform OA source apportionment on a case study event such as this. A number of different approaches to determining the optimal apportionment were tried and the one that yielded the most statistically optimal version treated as a 'best estimate', although it is acknowledged that even this may not be perfect. Indeed, it may not be possible to describe this data completely using the PMF data model. Six different tests were compared; four tests before modifying the fragmentation table and two tests when modifying the fragmentation table to determine a PON source. Test2_ON was the optimal 'best estimate' solution, a brief description is given here after being compared to the other tests (Section S7.2 in supplement). From this analysis, test2 resulted to be the best way to deconvolve OA sources, with the lowest parameters analysed: residuals, Q/Qexp values and Chi square. After modifying the fragmentation table, Test2_ON still shows a good performance with low parameters (Fig. S6-S8). Refer to section S7 in supplementary material for detailed information about source apportionment strategy and analysis performed to determine the optimal solution.

Comment [ERV8]: Paragraph edited in response to comment 1 of Referee 1.

Two steps were involved in Test2_ON: in step a, PMF/ME-2 were run for the event before and after the bonfire night (named as not bonfire event, nbf). In Step b, mass spectra from the solution identified in step a were used as TP, to analyse the bonfire-only (bfo) event. Finally, both solutions (nbf and bfo) were merged for further analysis. Different OA sources were identified in Test2_ON (Fig. 5), five sources were identified during nbf event: biomass burning OA (BBOA), hydrocarbon-like OA (HOA), cooking OA (COA), secondary particulate organic oxides of nitrogen (sPON_ME2) and low volatility OA (LVOOA). These sources are identified by characteristic peaks at their mass spectrum; BBOA, which is generated during the combustion of biomass, has a peak at m/z 60, related to levoglucosan (Alfarra et al., 2007); HOA, related to traffic emissions, presents high signals at m/z 55 and m/z 57 typical of aliphatic hydrocarbons (Canagaratna et al., 2004); COA, emitted from food cooking activities, is similar to HOA with a higher m/z 55 and lower m/z 57 (Allan et al.,

2010;Slowik et al., 2010;Mohr et al., 2012); LVOOA, identified as a secondary organic aerosol, has a high signal at m/z 44 dominated by the CO_2^+ ion (Ng et al., 2010); sPON_ME2 has a strong signal at m/z 30 and it has been identified to be secondary as it follows the same trend as LVOOA (Figure 5.a). In the case of the bfo event six different sources were identified: BBOA, HOA, COA, LVOOA and two factors with peaks at m/z30, which is related to PON (Sun et al., 2012). These two PON factors may have different sources; one may be secondary (sPON_ME2) and the other primary (pPON_ME2) which has similar trend as BBOA (Fig. 5.b). Further details about pPON_ME2 and sPON_ME2 nature will be explored in section 4.2.

Comment [ERV9]: Paragraph edited in response to comment 3 (1) of Referee 1.

Comment [ERV10]: Paragraph edited in response to the comment of Refere 2 related to explain more about the OA sources deconvolved with ME-2/PMF.

4. Discussion

4.1 OA source apportionment during bfo event.

It is worth noting that, while all sources have their characteristic peaks and no apparent mass spectral 'mixing' between sources (for example COA with signal at m/z 60), COA, HOA and LVOOA present high concentrations during the bonfire night (Fig. 5.b). High concentrations of these sources could expected as these (traffic and cooking activities) increase before and after the main bonfire events and the night represented a very strong inversion (which will trap all pollutants), but given the high concentrations experienced during the event and known variability for biomass burning emissions, the 'model error' and thus rotational freedom is likely to be substantial. The result is that these two factors could contain indeterminate contributions from minor variabilities within the biomass burning profile and therefore must be interpreted with caution.

b_{abs_470wb} has the same source as BBOA, thus the correlation between these two can be used to evaluate the effectivenes of BBOA deconvolution from OA concentrations (Frohlich et al., 2015;Visser et al., 2015). Here r^2 values are calculated for the bfo event between b_{abs_470wb} and the two BBOA's obtained; BBOA, obtained without modifying the fragmentation table and BBOA_2 obtained after modifying the fragmentation table to identify a PON factor. A higher correlation between b_{abs_470wb} and BBOA_2 was observed with r^2 = 0.880 compared to r^2 = 0.839 for b_{abs_470wb} and BBOA. This improvement on the BBOA_2 is explained by the fact that the PON factor may be mixed with BBOA and when both sources are separated a higher correlation between BBOA_2 and b_{abs_470wb} is present. There is the possibility the lower r^2 between b_{abs_470wb} and BBOA is due to having two BBOA factors in test2. However, an r^2=0.813 between b_{abs_470wb} and the sum of BBOA+BBOA_1 is still lower than 0.880.

Comment [ERV11]: Paragraph edited in response to comment 2 (4) of Referee 1.

Here is shown the importance of performing OA source apportionment using different approaches in order to identify the best way to deconvolve OA sources. PMF and ME-2 source apportionment tools could not completely deconvolve OA sources during the bfo event. However, due to the high correlation between for b_{abs_470wb} and BBOA_2 (r^2 = 0. 880) we consider that while BBOA_2 might not represent the total OA concentrations from the bonfire night event, it does represent the trend of OA emmited from the biomass burning.

Comment [ERV12]: Paragraph edited in response to comment 1 of Referee 1 and comment of Referee 2 related to PMF being pushed away to far in this manuscript.

4.2 PON Primary/secondary.

PON concentrations, obtained from the m/z ratios 46:30 (blue line in Fig. 6) have similar trend as BBOA, both increasing at the same time, suggesting a primary origin, but after 22:00 hrs, when BBOA concentrations drop, PON concentrations remain present with a slow decrease and maintaining low concentrations when BBOA concentrations were not present any more. This suggests the hypothesis that there might not be only one type of PON, and it could be divided into primary and secondary organic nitrate as reported in previous studies performed in western Europe (Mohr et al., 2013;Kiendler-Scharr et al., 2016).

Using this working hypothesis, primary and secondary PON concentrations were estimated using the slope between PON and BBOA, calculated from 18:00 – 12:00 hrs, time when the main bonfire night event took place (Fig. S10). PON concentrations were multiplied by this slope in order to calculate the primary organic nitrate (pPON) and secondary organic nitrate concentrations were calculated as: sPON = PON - pPON. Figure 6 shows the time series of this estimation where pPON reaches 2.5 ugm-3 and sPON with concentrations of 0.5 µg.m^{-3}.

A similar behaviour with two different PON sources was observed in the source apportionment analysis performed in section 3.3, where it was possible to separate two factors with a peak at m/z 30, characteristic of PON. Figure 7 shows that around 02:00 hrs, concentrations of the pPON_ME2 started to decrease (green line) while sPON_ME2 concentrations (grey line) increased. This analysis shows the presence of two different types of PON, pPON_ME2 is primarily emitted along with BBOA concentrations with the further presence of a different PON, considered to be secondary, due to its increase when primary pollutants start to decrease. Primary and secondary sources of PON have been previously identified from AMS-PMF analysis; Hao et al. (2014) identified PON to be secondary of nature, produced from the interaction between forest and urban emissions, while Zhang et al. (2016) determined PON to be related to primary combustion sources. In this study, is worth noticing that the increase of sPON_ME2 takes places around 2:00 hrs, a period when NO concentrations started decreasing and CIMS-measured N_2O_5 and $ClNO_2$ started to increase suggesting that nitrate radical chemistry was occurring (Fig. 8), which is possibly the source of the sPON, although the exact mechanism can only be speculated on.

Comment [ERV13]: Citations supporting primary and secondary origin of PON

This nitrogen chemistry process can be observed also in the gas phase, during the day, the main oxidants are O_3 and OH while the nitrate radical is unable to participate in daytime chemistry due to being rapidly photolyzed or reacting with NO to produce NO_2, (Ayres et al., 2015). Nitrate chemistry at night is important as nitrate radicals can be the main oxidants in polluted nocturnal environments away from enhanced NO and can create reservoirs and sinks of NO_x. The main NO_x removal at night is via the uptake of dinitrogen pentoxide (N_2O_5) into aerosols, as at night N_2O_5 is formed from NO_3 and NO_2. In the presence of chloride in the particle phase (e.g. in sea salt particles), N_2O_5 reacts to produce nitryl chloride ($ClNO_2$). In the morning, following overnight accumulation of $ClNO_2$, photochemical reactions take place to produce Cl and NO_2. N_2O_5 and $ClNO_2$ processing an interactions with nitrate chemistry has been previously studied in the UK (Le Breton et al., 2014a;Bannan et al., 2015). Figure 8 shows N_2O_5, $ClNO_2$ and O_3 concentrations increasing when NO and NO_2 concentrations decrease. All these processes may facilitate the sPON production at night. N_2O_5 concentrations reduce quickly after the sun rises, around 08:00 hours, while $ClNO_2$ concentrations decrease at a slower rate, with the lowest concentrations observed around 13:00 hours. Along with NO_3 chemistry, it was possible to observe other nitrogen containing gases during bonfire night using the CIMS such as hydrogen cyanide (HCN) and Nitrous acid (HONO), which have been found to be emitted from fires (Le Breton et al., 2013;Wang et al., 2015). High HONO concentrations at night are important during next morning when HONO reacts to produce OH and NO which impacts both the OH budget and NO_x concentrations early next morning (Lee et al., 2016).

4.3 OA factors and CIMS correlations

Analysing the CIMS measurements and comparing them with the OA factors, it may be possible to identify gas markers that can be used as inputs (target time series) to constrain solutions in future ME-2 analyses or as proxies when AMS data is not available. A linear regression was performed between the OA sources determined in section 3.4.1 and CIMS peaks that have been considered positively identified (Priestley et al., in preparation), performing a coefficient of determination (r^2) analysis for the complete dataset (ALL), and the event HSC, LC, bfo and WL. During the event HSC, none of the OA sources showed an r^2 higher than 0.6. HOA did not have an r^2 higher than 0.6 with any of the different events analysed. There were no specific markers identified for COA, while COA showed r^2 values higher than 0.6 for bfo event, these r^2's were observed also with BBOA even with higher values. Table S4 shows the r^2 values, higher or equal to 0.4, obtained in this analysis. It is

worth noting that r^2 values in ALL event seem to be influenced by the bfo event; this is the case for BBOA, COA and LVOOA which show similar r^2 values in both events. Thus, the analysis will be explained only in the individual events: bfo LC, and WL.

As expected, during bfo, BBOA is the OA source that shows the highest number of correlations during bonfire night. During bfo episode, high correlations (r^2) were observed with BBOA and methacrylic acid (0.92), Acrylic acid (0.90), nitrous acid (0.86), propionic acid, (0.85) and Hydrogen cyanide (0.76), which have been previously determined as biomass burning tracers (Veres et al., 2010;Le Breton et al., 2013). Formic acid presented a high correlation (r2=0.86) with BBOA during bonfire night, however this value drops to 0.52 for all the dataset, which suggests formic acid during bonfire night is mainly primary while formic acid concentrations measured for the whole dataset may be related to primary and secondary sources. This agrees with Le Breton et al. (2014b) who explored both primary and secondary origins of formic acid.

During the bfo event, LVOOA did not show a characteristic gas marker as all the r^2 values were also observed with BBOA. This suggests two hypotheses, that the LVOOA was mixed with BBOA, in the form of humic-like material (Paglione et al., 2014), which cannot be differentiated from secondary OA in the mass spectra (Fig. 5.c), or it could also be that secondary LVOOA may actually be present at the same time as BBOA concentrations, as it has been observed that during high relative humidity and low temperature enhanced partitioning of semi-volatile material to the particle phase occurs, where subsequent oxidation and oligomerisation may occur. Moreover, due to the high aerosol concentration present during the bonfire night, there is more surface available for gases to be condensed and more particulate bulk to absorb into, thus it could be speculated that there would be high secondary aerosol concentrations. However, this is deemed unlikely, as there is unlikely to be much gas phase oxidation occurring in the presence of such high NO concentrations, which will remove ozone and nitrate radicals, the main source of oxidants at night.

During the bfo event, pPON_ME2 showed high r^2 values with carbon monoxide (0.78) as well as hydrogen cyanide (0.77), Methylformamide (0.65) and Dimethylformamide (0.63) which are typical primary pollutants related to combustion processes [(Borduas et al., 2015) and references therein]. sPON_ME2 showed low correlations with $ClNO_2$ (0.52) and $ClNO_3$ (0.53). High r^2 values were also observed during LC episode between $ClNO_2$ - $ClNO_3$ and LVOOA (0.67 - 0.66) and sPON (0.74 - 0.69) proving their secondary origin. Cl_2, which has been previously identified to be related to both primary and secondary sources (Faxon et al., 2015), shows low correlations with pPON_ME2 (0.44) during bfo event and sPON_ME2 (0.55) during LC event.

Comment [ERV14]: Paragraph edited in response to comment 3 (1) of Referee 1 and comment of referee2 related to using I-CIMS tracers to correlate with pPON and sPON.

4.4 PON and its relationship with b_{abs_470wb} and BBOA

Comment [ERV15]: The r2 values described in the manuscript have been verified to match values in table 1. Comment 2 (1) Referee 1.

Organic oxides of nitrogen, originating from biomass burning, have been previously found to absorb light near the UV region (Jacobson, 1999;Flowers et al., 2010;Mohr et al., 2013). However, there is still a question of whether this absorption is due to primary or secondary PON. Here, the relationship between b_{abs_470wb} and PON and BBOA will be analysed to determine if sPON absorbs at 470 Mm^{-1}, which would interfere with Aethalometer measurements.

In order to quantitatively determine any contribution from organic nitrates to the Aethalometer data products, a multilinear regression (MLR) analysis was performed on the complete dataset dataset (ALL), and the events HSC, LC, bfo and WL (Table 1). This analysis was done in three ways: MLR 1 with BBOA from OA source apportionment without modifying the FragPanel and PON from m/z 46:30 analysis; MLR 2 with BBOA_2 from OA source apportionment after modifying the FragPanel and PON from 46:30 analysis; MLR 3 with with BBOA_2 and PON sources from OA source apportionment after modifying the FragPanel. The following bilinear regression was used:

$$b_{abs\_470wb} = A + B*x1 + C*x2 \quad (6)$$

When the parameter s"D" and x3 are used it means a trilinear regression was performed. MLR1 x1=BBOA, x2=PON. MLR2 x1=BBOA_2, x2=PON. MLR3 x1= BBOA_2, x2=sPON_ME2, x3=LVOOA in HSC and x3= pPON in bfo. A is the origin and the partial slopes B, C and D represent the contribution of x1 ,x2 and x3 to b_{abs_470wb}, respectively.

As used in previous studies (Elser et al., 2016;Reyes-Villegas et al., 2016), multilinear regression analysis allows to determine the relationship of one parameter between two or more variables. Here we are analysing the partial slopes and origin to determine the correlation of b_{abs_470wb} with the other variables. Table 1 shows the MLR outputs where; A represents the background, B, C and D represent the partial slope between b_{abs_470wb} and the respective organic aerosol. B/C represents the ratio between B and C partial slopes, with the following considerations: if B/C < 1 then, there is a higher contribution of organic nitrates to b_{abs_470wb}; if B/C > 1 then, there is a higher contribution of BBOA to b_{abs_470wb}. Looking at the coefficient of determination of the multilinear regression (r^2_MLR) for the three MLR analyses, it is possible to observe that HSC and LC events present low r^2_MLR values ranging from 0.064 and 0.480, while bfo and WL events have high correlations with values between 0.760 and 0.910, which shows that is during high primary OA emissions are present when a high correlation between b_{abs_470wb} and BBOA and PON is observeed.

Comment [ERV16]: Paragraph edited in response to comment 2 (2) of Referee 1.

These high r^2 values, particularly during the bfo event which presented the highest r^2 (0.910), are consistent with previous studies that found organic nitrates absorb at short wavelengths; Mohr et al. (2013) identified correlation values of 0.65 between nitrophenols and $babs_{370wb}$. Teich et al. (2017), in a recent study from offline filters, determined nitrated aerosol concentrations with further analysis of the light absorption of aqueous filter extracts ($babs_{370}$), identified r^2 values between b_{abs_370} and nitrated aerosol concentrations of 0.67 to 0.74 depending on acidic or alkaline conditions respectively.

In MLR 3, it is possible to observe that, during bfo event, the main contribution to b_{abs_470wb} is attribuited to both BBOA_2 (16.657) and pPON_ME2 (7.357) while babs:sPON_ME-2 values were zero, with an optimum r^2 of 0.910. This lack of correlation between babs and sPON is observed in the linear regression babs:sPON_ME2 with an r^2 of 0.188. These results show that while there is evidence of pPON_ME2 absorbing at 470 nm, with a partial slope of 16.657, sPON_ME2 did not show to be absorbing at 470 nm. The implication of the background not going to zero (6.093) is that there is still an unexplained contribution to the absorbtion at 470 nm, unreleated to sPON_ME2.

In order to further explore the possibility of sPON_ME-2 absorbing at 470 nm, the HSC event was analysed, where sPON_ME2 was shown to be non-absorbing at 470 nm with a partial slope of zero. On the other hand, BBOA_2 had a partial slope of 27.288 and bkgd a value of 2.527. This background value suggests there is another component related to b_{abs_470wb} that is not sPON. Thus, a trilinear regression was performed to *HSC between b_{abs_470wb} and BBOA_2, sPON and LVOOA. Here, the background value drops to 1.649, sPON partial slope is zero and LVOOA presents a partial slope of 1.138. These results confirm that sPON do not absorb light at 470 nm while LVOOA, or at least part of the components of LVOOA, absorb during the HSC event and pPON_ME2 absorbs during the bfo event.

These results agree with previous studies that found biomass burning OA contain important concentrations of light absorbing brown carbon (BrC) and that certain types of SOA are effective absorbers near UV light (Bones et al., 2010;Saleh et al., 2014;Washenfelder et al., 2015). The fact that pPON_ME2 and LVOOA were shown to be absorbing light at a short wavelength (470 nm) will have a direct impact on Aethalometer model studies; while pPON_ME2 could be considered a component of the wood burning aerosol apportioned using the Aethalometer, it may be that there is an interference from other forms of BrC in SOA. However, this work would suggest that sPON specifically does not contribute to the latter, so a different component of LV-OOA would have to be responsible. As well as Aethalometer interpretation, it is also worth mentioning that these findings may have implications for studies on the radiative properties of the atmosphere, as BrC is also thought to affect climate (Jacobson, 2014).

Comment [ERV17]: Citation added in response to minor comment 4 Referee 1.

5. Conclusions

In order to better understand the aerosol chemical composition and variation in source contribution during periods of nocturnal pollution, online measurements of gases and aerosols were made in ambient air between 29th October and 10th November 2014, at the University of Manchester with detailed analysis of the special high pollutant concentrations during bonfire night celebrations on 5th November. High aerosol concentrations were observed during the bonfire night event with 115 µg.m^{-3} of PM_1. Important nitrogen chemistry was present with high HCN, HCNO and HONO concentrations primarily emitted with further presence of N_2O_5 and $ClNO_2$ concentrations from nocturnal nitrate chemistry taking place after NO_x concentrations decreased.

Organic aerosol source apportionment was performed using the ME-2 factorisation tool. The particular high pollutant concentrations together with the complex mix of emissions did not allow the running of ME-2 for the complete dataset, thus the dataset was divided into different event s. The best way to perform source apportionment was found to be to, (a) analyse the event before and after the bonfire night using BBOA, HOA and COA from a previous study in Paris as TP, and (b) conduct a further ME-2 analysis of the bonfire night event using BBOA, HOA and COA mass spectra from (a) as TP. Moreover, an improvement on the source apportionment was observed after modifying the fragPanel in order to identify organic nitrate sources, increasing the r^2 value from linear regressions between b_{abs_470wb} (absorption coefficient of wood burning at 470 nm) and BBOA from 0.839 to 0.880. PMF and ME-2 source apportionment tools could not completely deconvolve OA sources during the bfo event as LV-OOA, COA and HOA may be mixed with BBOA concentrations. However, due to the high correlation between for b_{abs_470wb} and BBOA (r^2 = 0. 880) we consider that while BBOA might not represent the total OA concentrations from the bonfire night event, it does represent the trend of OA emmited from the biomass burning.

Comment [ERV18]: Paragraph edited from comment 1 of Referee 1.

The combination of CIMS measurements and OA sources determined from AMS measurements provided important information about gas tracers to be used as inputs (target time series) to improve future ME-2 analyses, particularly gases correlating with BBOA, LVOOA and secondary particulate organic nitrate. However the use of these species as target time series should be used with care as their time variation are greatly affected by meteorological conditions.

The presence of two classes of particulate organic nitrate (PON), secondary (sPON_ME2) and primary (pPON_ME2) PON, was identified both from looking at the BBOA:PON relationship and from the ME-2 analysis after modifying the FragPanel. It is clear that, during bonfire night, pPON_ME2 concentrations increased when BBOA concentrations are present and sPON_ME2 concentrations started evolving when the primary concentrations decreased.

It was determined that pPON_ME2 absorbed light at a wavelenght of 470 nm during the bonfire night, where the multilinear regression perfomed between b_{abs_470wb}, BBOA and pPON_ME2 showed a high r^2 of 0.910 while sPON_ME2 did not contribute to light absorption at 470nm. During the HSC episode, LVOOA showed a partial slope of 1.138 in the multilinear regression and an r^2 from linear regression with b_{abs_470wb} of 0.225, implying secondary LVOOA (associated with SOA) may be absorbing at 470 nm and sPON_ME2 was not absorbing at this wavelength. These results will help us to understand the mechanistic contributions to UV absorption in the Aethalometer and will have direct implications for source apportionment studies, which may need to be corrected for secondary organic aerosol interferences near the UV region.

6. Data availability

Processed data is available through the archive at the British Atmospheric Data Centre (http://badc.nerc.ac.uk/browse/badc), with search term `COMPART'. Raw data is archived at the University of Manchester and is available on request.

Author contributions. Ernesto Reyes-Villegas, Michael Flynn, Hugh Coe, Carl Percival, James Allan designed the project; Ernesto Reyes-Villegas, Yu-Chieh Ting, Sophie Haslett, Thomas Bannan, Michael Le breton, Paul Williams, Asan Bacak, operated, calibrated and performed QA of instrument measurements; Ernesto Reyes-Villegas and Michael Priestley performed the data analysis; Ernesto Reyes-Villegas, Hugh Coe and James Allan wrote the paper.

Acknowledgements. This work was supported through the UK Natural Environment Research Council (NERC) through the Com-Part (grant ref: NE/K014838/1). Ernesto Reyes-Villegas is supported by a studentship by the National Council of Science and Technology-Mexico (CONACYT) under registry number 217687.

References

Ainsworth, W. H.: Guy fawkes; or, the gunpowder treason, Nottingham Society, 1850.

Alfarra, M. R., Paulsen, D., Gysel, M., Garforth, A. A., Dommen, J., Prévôt, A. S. H., Worsnop, D. R., Baltensperger, U., and Coe, H.: A mass spectrometric study of secondary organic aerosols formed from the photooxidation of anthropogenic and biogenic precursors in a reaction chamber, Atmos Chem Phys, 6, 5279-5293, 2006.

Alfarra, M. R., Prevot, A. S. H., Szidat, S., Sandradewi, J., Weimer, S., Lanz, V. A., Schreiber, D., Mohr, M., and Baltensperger, U.: Identification of the mass spectral signature of organic aerosols from wood burning emissions, Environmental Science & Technology, 41, 5770-5777, Doi 10.1021/Es062289b, 2007.

Allan, J. D., Delia, A. E., Coe, H., Bower, K. N., Alfarra, M. R., Jimenez, J. L., Middlebrook, A. M., Drewnick, F., Onasch, T. B., Canagaratna, M. R., Jayne, J. T., and Worsnop, D. R.: A generalised method for the extraction of chemically resolved mass spectra from aerodyne aerosol mass spectrometer data, J Aerosol Sci, 35, 909-922, DOI 10.1016/j.jaerosci.2004.02.007, 2004.

Allan, J. D., Alfarra, M. R., Bower, K. N., Coe, H., Jayne, J. T., Worsnop, D. R., Aalto, P. P., Kulmala, M., Hyötyläinen, T., Cavalli, F., and Laaksonen, A.: Size and composition measurements of background aerosol and new particle growth in a finnish forest during quest 2 using an aerodyne aerosol mass spectrometer, Atmos. Chem. Phys., 6, 315-327, 10.5194/acp-6-315-2006, 2006.

Allan, J. D., Williams, P. I., Morgan, W. T., Martin, C. L., Flynn, M. J., Lee, J., Nemitz, E., Phillips, G. J., Gallagher, M. W., and Coe, H.: Contributions from transport, solid fuel burning and cooking to primary organic aerosols in two uk cities, Atmos Chem Phys, 10, 647-668, 2010.

Ayres, B. R., Allen, H. M., Draper, D. C., Brown, S. S., Wild, R. J., Jimenez, J. L., Day, D. A., Campuzano-Jost, P., Hu, W., de Gouw, J., Koss, A., Cohen, R. C., Duffey, K. C., Romer, P., Baumann, K., Edgerton, E., Takahama, S., Thornton, J. A., Lee, B. H., Lopez-Hilfiker, F. D., Mohr, C., Wennberg, P. O., Nguyen, T. B., Teng, A., Goldstein, A. H., Olson, K., and Fry, J. L.: Organic nitrate aerosol formation via no3 + biogenic volatile organic compounds in the southeastern united states, Atmos. Chem. Phys., 15, 13377-13392, 10.5194/acp-15-13377-2015, 2015.

Bannan, T. J., Booth, A. M., Bacak, A., Muller, J. B. A., Leather, K. E., Le Breton, M., Jones, B., Young, D., Coe, H., Allan, J., Visser, S., Slowik, J. G., Furger, M., Prevot, A. S. H., Lee, J., Dunmore, R. E., Hopkins, J. R., Hamilton, J. F., Lewis, A. C., Whalley, L. K., Sharp, T., Stone, D., Heard, D. E., Fleming, Z. L., Leigh, R., Shallcross, D. E., and Percival, C. J.: The first uk measurements of nitryl chloride using a chemical ionization mass spectrometer in central london in the summer of 2012, and an investigation of the role of cl atom oxidation, J Geophys Res-Atmos, 120, 5638-5657, 10.1002/2014JD022629, 2015.

Bones, D. L., Henricksen, D. K., Mang, S. A., Gonsior, M., Bateman, A. P., Nguyen, T. B., Cooper, W. J., and Nizkorodov, S. A.: Appearance of strong absorbers and fluorophores in limonene-o3 secondary organic aerosol due to nh4+-mediated chemical aging over long time scales, Journal of Geophysical Research: Atmospheres, 115, n/a-n/a, 10.1029/2009jd012864, 2010.

Borduas, N., da Silva, G., Murphy, J. G., and Abbatt, J. P. D.: Experimental and theoretical understanding of the gas phase oxidation of atmospheric amides with oh radicals: Kinetics, products, and mechanisms, The Journal of Physical Chemistry A, 119, 4298-4308, 10.1021/jp503759f, 2015.

Bruns, E. A., Perraud, V., Zelenyuk, A., Ezell, M. J., Johnson, S. N., Yu, Y., Imre, D., Finlayson-Pitts, B. J., and Alexander, M. L.: Comparison of ftir and particle mass spectrometry for the measurement of particulate organic nitrates, Environmental Science & Technology, 44, 1056-1061, 10.1021/es9029864, 2010.

Canagaratna, M. R., Jayne, J. T., Ghertner, D. A., Herndon, S., Shi, Q., Jimenez, J. L., Silva, P. J., Williams, P., Lanni, T., Drewnick, F., Demerjian, K. L., Kolb, C. E., and Worsnop, D. R.: Chase studies of particulate emissions from in-use new york city vehicles, Aerosol Science and Technology, 38, 555-573, 10.1080/02786820490465504, 2004.

Canonaco, F., Crippa, M., Slowik, J. G., Baltensperger, U., and Prevot, A. S. H.: Sofi, an igor-based interface for the efficient use of the generalized multilinear engine (me-2) for the source apportionment: Me-2 application to aerosol mass spectrometer data, Atmos Meas Tech, 6, 3649-3661, DOI 10.5194/amt-6-3649-2013, 2013.

Chakraborty, A., Gupta, T., and Tripathi, S. N.: Chemical composition and characteristics of ambient aerosols and rainwater residues during indian summer monsoon: Insight from aerosol mass spectrometry, Atmos Environ, 136, 144-155, 10.1016/j.atmosenv.2016.04.024, 2016.

Clark, H.: New directions. Light blue touch paper and retire, Atmos Environ, 31, 2893-2894, 10.1016/s1352-2310(97)88278-7, 1997.

Colbeck, I., and Chung, M.-C.: Ambient aerosol concentrations at a site in se england during bonfire night 1995, J Aerosol Sci, 27, Supplement 1, S449-S450, http://dx.doi.org/10.1016/0021-8502(96)00297-2, 1996.

Crilley, L. R., Bloss, W. J., Yin, J., Beddows, D. C. S., Harrison, R. M., Allan, J. D., Young, D. E., Flynn, M., Williams, P., Zotter, P., Prevot, A. S. H., Heal, M. R., Barlow, J. F., Halios, C. H., Lee, J. D., Szidat, S., and Mohr, C.: Sources and contributions of wood smoke during winter in london: Assessing local and regional influences, Atmos. Chem. Phys., 15, 3149-3171, 10.5194/acp-15-3149-2015, 2015.

Crippa, M., DeCarlo, P. F., Slowik, J. G., Mohr, C., Heringa, M. F., Chirico, R., Poulain, L., Freutel, F., Sciare, J., Cozic, J., Di Marco, C. F., Elsasser, M., Nicolas, J. B., Marchand, N., Abidi, E., Wiedensohler, A., Drewnick, F., Schneider, J., Borrmann, S., Nemitz, E., Zimmermann, R., Jaffrezo, J. L., Prevot, A. S. H., and Baltensperger, U.: Wintertime aerosol chemical composition and source apportionment of the organic fraction in the metropolitan area of paris, Atmos Chem Phys, 13, 961-981, DOI 10.5194/acp-13-961-2013, 2013.

Crippa, M., Canonaco, F., Lanz, V. A., Aijala, M., Allan, J. D., Carbone, S., Capes, G., Ceburnis, D., Dall'Osto, M., Day, D. A., DeCarlo, P. F., Ehn, M., Eriksson, A., Freney, E., Ruiz, L. H., Hillamo, R., Jimenez, J. L., Junninen, H., Kiendler-Scharr, A., Kortelainen, A. M., Kulmala, M., Laaksonen, A., Mensah, A., Mohr, C., Nemitz, E., O'Dowd, C., Ovadnevaite, J., Pandis, S. N., Petaja, T., Poulain, L., Saarikoski, S., Sellegri, K., Swietlicki, E., Tiitta, P., Worsnop, D. R., Baltensperger, U., and Prevot, A. S. H.: Organic aerosol components derived from 25 ams data sets across europe using a consistent me-2 based source apportionment approach, Atmos Chem Phys, 14, 6159-6176, DOI 10.5194/acp-14-6159-2014, 2014.

Day, D. A., Liu, S., Russell, L. M., and Ziemann, P. J.: Organonitrate group concentrations in submicron particles with high nitrate and organic fractions in coastal southern california, Atmos Environ, 44, 1970-1979, http://dx.doi.org/10.1016/j.atmosenv.2010.02.045, 2010.

Drewnick, F., Hings, S. S., DeCarlo, P., Jayne, J. T., Gonin, M., Fuhrer, K., Weimer, S., Jimenez, J. L., Demerjian, K. L., Borrmann, S., and Worsnop, D. R.: A new time-of-flight aerosol mass spectrometer (tof-ams) - instrument description and first field deployment, Aerosol Science and Technology, 39, 637-658, Doi 10.1080/02786820500182040, 2005.

Drewnick, F., Hings, S. S., Curtius, J., Eerdekens, G., and Williams, J.: Measurement of fine particulate and gas-phase species during the new year's fireworks 2005 in mainz, germany, Atmos Environ, 40, 4316-4327, http://dx.doi.org/10.1016/j.atmosenv.2006.03.040, 2006.

Drewnick, F., Diesch, J. M., Faber, P., and Borrmann, S.: Aerosol mass spectrometry: Particle–vaporizer interactions and their consequences for the measurements, Atmos. Meas. Tech., 8, 3811-3830, 10.5194/amt-8-3811-2015, 2015.

Dyke, P., Coleman, P., and James, R.: Dioxins in ambient air, bonfire night 1994, Chemosphere, 34, 1191-1201, http://dx.doi.org/10.1016/S0045-6535(97)00418-9, 1997.

EEA: Status of black carbon monitoring in ambient air in europe, 48, 2013.

Elser, M., Huang, R. J., Wolf, R., Slowik, J. G., Wang, Q., Canonaco, F., Li, G., Bozzetti, C., Daellenbach, K. R., Huang, Y., Zhang, R., Li, Z., Cao, J., Baltensperger, U., El-Haddad, I., and André, P.: New insights into pm2.5 chemical composition and sources in two major cities in china during extreme haze events using aerosol mass spectrometry, Atmos Chem Phys, 16, 3207-3225, 10.5194/acp-16-3207-2016, 2016.

Faber, P., Drewnick, F., Veres, P. R., Williams, J., and Borrmann, S.: Anthropogenic sources of aerosol particles in a football stadium: Real-time characterization of emissions from cigarette smoking, cooking, hand flares, and color smoke bombs by high-resolution aerosol mass spectrometry, Atmos Environ, 77, 1043-1051, DOI 10.1016/j.atmosenv.2013.05.072, 2013.

Farmer, D. K., Matsunaga, A., Docherty, K. S., Surratt, J. D., Seinfeld, J. H., Ziemann, P. J., and Jimenez, J. L.: Response of an aerosol mass spectrometer to organonitrates and organosulfates and implications for

atmospheric chemistry, Proceedings of the National Academy of Sciences of the United States of America, 107, 6670-6675, 10.1073/pnas.0912340107, 2010.
Farrar, N. J., Smith, K. E. C., Lee, R. G. M., Thomas, G. O., Sweetman, A. J., and Jones, K. C.: Atmospheric emissions of polybrominated diphenyl ethers and other persistent organic pollutants during a major anthropogenic combustion event, Environmental Science & Technology, 38, 1681-1685, 10.1021/es035127d, 2004.
Faxon, C., Bean, J., and Ruiz, L.: Inland concentrations of cl2 and clno2 in southeast texas suggest chlorine chemistry significantly contributes to atmospheric reactivity, Atmosphere, 6, 1487, 2015.
Fernandez, P., Grifoll, M., Solanas, A. M., Bayona, J. M., and Albaiges, J.: Bioassay-directed chemical analysis of genotoxic components in coastal sediments, Environmental Science & Technology, 26, 817-829, 10.1021/es00028a024, 1992.
Florou, K., Papanastasiou, D. K., Pikridas, M., Kaltsonoudis, C., Louvaris, E., Gkatzelis, G. I., Patoulias, D., Mihalopoulos, N., and Pandis, S. N.: The contribution of wood burning and other pollution sources to wintertime organic aerosol levels in two greek cities, Atmos. Chem. Phys., 17, 3145-3163, 10.5194/acp-17-3145-2017, 2017.
Flowers, B. A., Dubey, M. K., Mazzoleni, C., Stone, E. A., Schauer, J. J., Kim, S. W., and Yoon, S. C.: Optical-chemical-microphysical relationships and closure studies for mixed carbonaceous aerosols observed at jeju island; 3-laser photoacoustic spectrometer, particle sizing, and filter analysis, Atmos. Chem. Phys., 10, 10387-10398, 10.5194/acp-10-10387-2010, 2010.
Frohlich, R., Crenn, V., Setyan, A., Belis, C. A., Canonaco, F., Favez, O., Riffault, V., Slowik, J. G., Aas, W., Aijala, M., Alastuey, A., Artinano, B., Bonnaire, N., Bozzetti, C., Bressi, M., Carbone, C., Coz, E., Croteau, P. L., Cubison, M. J., Esser-Gietl, J. K., Green, D. C., Gros, V., Heikkinen, L., Herrmann, H., Jayne, J. T., Lunder, C. R., Minguillon, M. C., Mocnik, G., O'Dowd, C. D., Ovadnevaite, J., Petralia, E., Poulain, L., Priestman, M., Ripoll, A., Sarda-Esteve, R., Wiedensohler, A., Baltensperger, U., Sciare, J., and Prevot, A. S. H.: Actris acsm intercomparison - part 2: Intercomparison of me-2 organic source apportionment results from 15 individual, co-located aerosol mass spectrometers, Atmos Meas Tech, 8, 2555-2576, 10.5194/amt-8-2555-2015, 2015.
Fry, J. L., Kiendler-Scharr, A., Rollins, A. W., Wooldridge, P. J., Brown, S. S., Fuchs, H., Dubé, W., Mensah, A., dal Maso, M., Tillmann, R., Dorn, H. P., Brauers, T., and Cohen, R. C.: Organic nitrate and secondary organic aerosol yield from no3 oxidation of β-pinene evaluated using a gas-phase kinetics/aerosol partitioning model, Atmos. Chem. Phys., 9, 1431-1449, 10.5194/acp-9-1431-2009, 2009.
Godri, K. J., Green, D. C., Fuller, G. W., Dall'Osto, M., Beddows, D. C., Kelly, F. J., Harrison, R. M., and Mudway, I. S.: Particulate oxidative burden associated with firework activity, Environmental Science & Technology, 44, 8295-8301, 10.1021/es1016284, 2010.
Hamad, S., Green, D., and Heo, J.: Evaluation of health risk associated with fireworks activity at central london, Air Quality, Atmosphere & Health, 1-7, 10.1007/s11869-015-0384-x, 2015.
Hao, L. Q., Kortelainen, A., Romakkaniemi, S., Portin, H., Jaatinen, A., Leskinen, A., Komppula, M., Miettinen, P., Sueper, D., Pajunoja, A., Smith, J. N., Lehtinen, K. E. J., Worsnop, D. R., Laaksonen, A., and Virtanen, A.: Atmospheric submicron aerosol composition and particulate organic nitrate formation in a boreal forestland-urban mixed region, Atmos Chem Phys, 14, 13483-13495, 10.5194/acp-14-13483-2014, 2014.
Harrison, M. A. J., Barra, S., Borghesi, D., Vione, D., Arsene, C., and Iulian Olariu, R.: Nitrated phenols in the atmosphere: A review, Atmos Environ, 39, 231-248, http://dx.doi.org/10.1016/j.atmosenv.2004.09.044, 2005.
Harrison, R. M., Beddows, D. C. S., Hu, L., and Yin, J.: Comparison of methods for evaluation of wood smoke and estimation of uk ambient concentrations, Atmos Chem Phys, 12, 8271-8283, DOI 10.5194/acp-12-8271-2012, 2012.
Jacobson, M. Z.: Isolating nitrated and aromatic aerosols and nitrated aromatic gases as sources of ultraviolet light absorption, J Geophys Res-Atmos, 104, 3527-3542, Doi 10.1029/1998jd100054, 1999.
Jacobson, M. Z.: Effects of biomass burning on climate, accounting for heat and moisture fluxes, black and brown carbon, and cloud absorption effects, Journal of Geophysical Research: Atmospheres, 119, 8980-9002, 10.1002/2014jd021861, 2014.
Joshi, M., Khan, A., Anand, S., and Sapra, B. K.: Size evolution of ultrafine particles: Differential signatures of normal and episodic events, Environmental Pollution, 208, Part B, 354-360, http://dx.doi.org/10.1016/j.envpol.2015.10.001, 2016.
Kiendler-Scharr, A., Mensah, A. A., Friese, E., Topping, D., Nemitz, E., Prevot, A. S. H., Äijälä, M., Allan, J., Canonaco, F., Canagaratna, M., Carbone, S., Crippa, M., Dall Osto, M., Day, D. A., De Carlo, P., Di Marco, C. F., Elbern, H., Eriksson, A., Freney, E., Hao, L., Herrmann, H., Hildebrandt, L., Hillamo, R., Jimenez, J. L., Laaksonen,

A., McFiggans, G., Mohr, C., O'Dowd, C., Otjes, R., Ovadnevaite, J., Pandis, S. N., Poulain, L., Schlag, P., Sellegri, K., Swietlicki, E., Tiitta, P., Vermeulen, A., Wahner, A., Worsnop, D., and Wu, H. C.: Ubiquity of organic nitrates from nighttime chemistry in the european submicron aerosol, Geophys Res Lett, 43, 7735-7744, 10.1002/2016gl069239, 2016.

Kitanovski, Z., Grgic, I., Vermeylen, R., Claeys, M., and Maenhaut, W.: Liquid chromatography tandem mass spectrometry method for characterization of monoaromatic nitro-compounds in atmospheric particulate matter, J Chromatogr A, 1268, 35-43, 10.1016/j.chroma.2012.10.021, 2012.

Kostenidou, E., Florou, K., Kaltsonoudis, C., Tsiflikiotou, M., Vratolis, S., Eleftheriadis, K., and Pandis, S. N.: Sources and chemical characterization of organic aerosol during the summer in the eastern mediterranean, Atmos. Chem. Phys., 15, 11355-11371, 10.5194/acp-15-11355-2015, 2015.

LASKAR, S. I., JASWAL, K., BHATNAGAR, M. K., and RATHORE, L. S.: India meteorological department, India, 1021-1037, 2016.

Le Breton, M., Bacak, A., Muller, J. B. A., O'Shea, S. J., Xiao, P., Ashfold, M. N. R., Cooke, M. C., Batt, R., Shallcross, D. E., Oram, D. E., Forster, G., Bauguitte, S. J. B., Palmer, P. I., Parrington, M., Lewis, A. C., Lee, J. D., and Percival, C. J.: Airborne hydrogen cyanide measurements using a chemical ionisation mass spectrometer for the plume identification of biomass burning forest fires, Atmos. Chem. Phys., 13, 9217-9232, 10.5194/acp-13-9217-2013, 2013.

Le Breton, M., Bacak, A., Muller, J. B. A., Bannan, T. J., Kennedy, O., Ouyang, B., Xiao, P., Bauguitte, S. J. B., Shallcross, D. E., Jones, R. L., Daniels, M. J. S., Ball, S. M., and Percival, C. J.: The first airborne comparison of n2o5 measurements over the uk using a cims and bbceas during the ronoco campaign, Anal Methods-Uk, 6, 9731-9743, 10.1039/c4ay02273d, 2014a.

Le Breton, M., Bacak, A., Muller, J. B. A., Xiao, P., Shallcross, B. M. A., Batt, R., Cooke, M. C., Shallcross, D. E., Bauguitte, S. J. B., and Percival, C. J.: Simultaneous airborne nitric acid and formic acid measurements using a chemical ionization mass spectrometer around the uk: Analysis of primary and secondary production pathways, Atmos Environ, 83, 166-175, http://dx.doi.org/10.1016/j.atmosenv.2013.10.008, 2014b.

Lee, B. H., Lopez-Hilfiker, F. D., Mohr, C., Kurtén, T., Worsnop, D. R., and Thornton, J. A.: An iodide-adduct high-resolution time-of-flight chemical-ionization mass spectrometer: Application to atmospheric inorganic and organic compounds, Environmental Science & Technology, 48, 6309-6317, 10.1021/es500362a, 2014.

Lee, J. D., Whalley, L. K., Heard, D. E., Stone, D., Dunmore, R. E., Hamilton, J. F., Young, D. E., Allan, J. D., Laufs, S., and Kleffmann, J.: Detailed budget analysis of hono in central london reveals a missing daytime source, Atmos. Chem. Phys., 16, 2747-2764, 10.5194/acp-16-2747-2016, 2016.

Liu, D., Whitehead, J., Alfarra, M. R., Reyes-Villegas, E., Spracklen, D. V., Reddington, C. L., Kong, S., Williams, P. I., Ting, Y.-C., Haslett, S., Taylor, J. W., Flynn, M. J., Morgan, W. T., McFiggans, G., Coe, H., and Allan, J. D.: Black-carbon absorption enhancement in the atmosphere determined by particle mixing state, Nature Geosci, 10, 184-188, 10.1038/ngeo2901, 2017.

Mao, J., Paulot, F., Jacob, D. J., Cohen, R. C., Crounse, J. D., Wennberg, P. O., Keller, C. A., Hudman, R. C., Barkley, M. P., and Horowitz, L. W.: Ozone and organic nitrates over the eastern united states: Sensitivity to isoprene chemistry, Journal of Geophysical Research Atmospheres, 118, 11256-11268, 10.1002/jgrd.50817, 2013.

Mohr, C., DeCarlo, P. F., Heringa, M. F., Chirico, R., Slowik, J. G., Richter, R., Reche, C., Alastuey, A., Querol, X., Seco, R., Penuelas, J., Jimenez, J. L., Crippa, M., Zimmermann, R., Baltensperger, U., and Prevot, A. S. H.: Identification and quantification of organic aerosol from cooking and other sources in barcelona using aerosol mass spectrometer data, Atmos Chem Phys, 12, 1649-1665, DOI 10.5194/acp-12-1649-2012, 2012.

Mohr, C., Lopez-Hilfiker, F. D., Zotter, P., Prevot, A. S. H., Xu, L., Ng, N. L., Herndon, S. C., Williams, L. R., Franklin, J. P., Zahniser, M. S., Worsnop, D. R., Knighton, W. B., Aiken, A. C., Gorkowski, K. J., Dubey, M. K., Allan, J. D., and Thornton, J. A.: Contribution of nitrated phenols to wood burning brown carbon light absorption in detling, united kingdom during winter time, Environmental Science & Technology, 47, 6316-6324, Doi 10.1021/Es400683v, 2013.

Moreno, T., Querol, X., Alastuey, A., Cruz Minguillón, M., Pey, J., Rodriguez, S., Vicente Miró, J., Felis, C., and Gibbons, W.: Recreational atmospheric pollution episodes: Inhalable metalliferous particles from firework displays, Atmos Environ, 41, 913-922, http://dx.doi.org/10.1016/j.atmosenv.2006.09.019, 2007.

Naeher, L. P., Brauer, M., Lipsett, M., Zelikoff, J. T., Simpson, C. D., Koenig, J. Q., and Smith, K. R.: Woodsmoke health effects: A review, Inhalation Toxicology, 19, 67-106, 10.1080/08958370600985875, 2007.

Ng, N. L., Canagaratna, M. R., Zhang, Q., Jimenez, J. L., Tian, J., Ulbrich, I. M., Kroll, J. H., Docherty, K. S., Chhabra, P. S., Bahreini, R., Murphy, S. M., Seinfeld, J. H., Hildebrandt, L., Donahue, N. M., DeCarlo, P. F., Lanz, V. A.,

Prevot, A. S. H., Dinar, E., Rudich, Y., and Worsnop, D. R.: Organic aerosol components observed in northern hemispheric datasets from aerosol mass spectrometry, Atmos Chem Phys, 10, 4625-4641, DOI 10.5194/acp-10-4625-2010, 2010.

Ng, N. L., Brown, S. S., Archibald, A. T., Atlas, E., Cohen, R. C., Crowley, J. N., Day, D. A., Donahue, N. M., Fry, J. L., Fuchs, H., Griffin, R. J., Guzman, M. I., Herrmann, H., Hodzic, A., Iinuma, Y., Kiendler-Scharr, A., Lee, B. H., Luecken, D. J., Mao, J., McLaren, R., Mutzel, A., Osthoff, H. D., Ouyang, B., Picquet-Varrault, B., Platt, U., Pye, H. O. T., Rudich, Y., Schwantes, R. H., Shiraiwa, M., Stutz, J., Thornton, J. A., Tilgner, A., Williams, B. J., and Zaveri, R. A.: Nitrate radicals and biogenic volatile organic compounds: Oxidation, mechanisms, and organic aerosol, Atmos Chem Phys, 17, 2103-2162, 10.5194/acp-17-2103-2017, 2017.

Paatero, P., and Tapper, U.: Positive matrix factorization: A non-negative factor model with optimal utilization of error estimates of data values, Environmetrics, 5, 111-126, 1994.

Paatero, P.: The multilinear engine: A table-driven, least squares program for solving multilinear problems, including the n-way parallel factor analysis model, J Comput Graph Stat, 8, 854-888, 10.2307/1390831, 1999.

Paglione, M., Kiendler-Scharr, A., Mensah, A. A., Finessi, E., Giulianelli, L., Sandrini, S., Facchini, M. C., Fuzzi, S., Schlag, P., Piazzalunga, A., Tagliavini, E., Henzing, J. S., and Decesari, S.: Identification of humic-like substances (hulis) in oxygenated organic aerosols using nmr and ams factor analyses and liquid chromatographic techniques, Atmos Chem Phys, 14, 25-45, DOI 10.5194/acp-14-25-2014, 2014.

Perring, A. E., Pusede, S. E., and Cohen, R. C.: An observational perspective on the atmospheric impacts of alkyl and multifunctional nitrates on ozone and secondary organic aerosol, Chemical Reviews, 113, 5848-5870, 10.1021/cr300520x, 2013.

Pervez, S., Chakrabarty, R. K., Dewangan, S., Watson, J. G., Chow, J. C., and Matawle, J. L.: Chemical speciation of aerosols and air quality degradation during the festival of lights (diwali), Atmospheric Pollution Research, 7, 92-99, 10.1016/j.apr.2015.09.002, 2016.

Petzold, A., Kramer, H., and Schonlinner, M.: Continuous measurement of atmospheric black carbon using a multi-angle absorption photometer, Environ Sci Pollut R, 78-82, 2002.

Priestley, M., Le Breton, M., Bannan, T. J., Leather, K. E., Bacak, A., Allan, J. D., Brazier, T., Reyes-Villegas, E., Shallcross, B. M. A., Khan, M. A., De Vocht, F., D.E., S., Coe, H., and Percival, C. J.: Manchester, uk bonfire night 2014: Air quality and emission ratios during an anthropogenic biomass burning event using a time of flight chemical ionisation mass spectrometer, In preparation.

Qingguo, H., Liansheng, W., and Shuokui, H.: The genotoxicity of substituted nitrobenzenes and the quantitative structure-activity relationship studies, Chemosphere, 30, 915-923, 10.1016/0045-6535(94)00450-9, 1995.

Ravindra, K., Mor, S., and Kaushik, C. P.: Short-term variation in air quality associated with firework events: A case study, Journal of Environmental Monitoring, 5, 260-264, 10.1039/b211943a, 2003.

Reyes-Villegas, E., Green, D. C., Priestman, M., Canonaco, F., Coe, H., Prévôt, A. S. H., and Allan, J. D.: Organic aerosol source apportionment in london 2013 with me-2: Exploring the solution space with annual and seasonal analysis, Atmos. Chem. Phys., 16, 15545-15559, 10.5194/acp-16-15545-2016, 2016.

Saleh, R., Robinson, E. S., Tkacik, D. S., Ahern, A. T., Liu, S., Aiken, A. C., Sullivan, R. C., Presto, A. A., Dubey, M. K., Yokelson, R. J., Donahue, N. M., and Robinson, A. L.: Brownness of organics in aerosols from biomass burning linked to their black carbon content, Nat Geosci, 7, 647-650, 10.1038/NGEO2220, 2014.

Sandradewi, J., Prévôt, A. S. H., Szidat, S., Perron, N., Alfarra, M. R., Lanz, V. A., Weingartner, E., and Baltensperger, U. R. S.: Using aerosol light abosrption measurements for the quantitative determination of wood burning and traffic emission contribution to particulate matter, Environmental Science and Technology, 42, 3316-3323, 10.1021/es702253m, 2008.

Sato, K., Takami, A., Isozaki, T., Hikida, T., Shimono, A., and Imamura, T.: Mass spectrometric study of secondary organic aerosol formed from the photo-oxidation of aromatic hydrocarbons, Atmos Environ, 44, 1080-1087, 10.1016/j.atmosenv.2009.12.013, 2010.

Slowik, J. G., Vlasenko, A., McGuire, M., Evans, G. J., and Abbatt, J. P.: Simultaneous factor analysis of organic particle and gas mass spectra: Ams and ptr-ms measurements at an urban site, Atmos Chem Phys, 10, 1969-1988, 2010.

Sun, Y. L., Zhang, Q., Schwab, J. J., Yang, T., Ng, N. L., and Demerjian, K. L.: Factor analysis of combined organic and inorganic aerosol mass spectra from high resolution aerosol mass spectrometer measurements, Atmos Chem Phys, 12, 8537-8551, DOI 10.5194/acp-12-8537-2012, 2012.

Teich, M., van Pinxteren, D., Wang, M., Kecorius, S., Wang, Z., Müller, T., Močnik, G., and Herrmann, H.: Contributions of nitrated aromatic compounds to the light absorption of water-soluble and particulate brown

carbon in different atmospheric environments in germany and china, Atmos. Chem. Phys., 17, 1653-1672, 10.5194/acp-17-1653-2017, 2017.
Tian, Y. Z., Wang, J., Peng, X., Shi, G. L., and Feng, Y. C.: Estimation of the direct and indirect impacts of fireworks on the physicochemical characteristics of atmospheric pm10 and pm2.5, Atmos Chem Phys, 14, 9469-9479, 10.5194/acp-14-9469-2014, 2014.
Tiitta, P., Leskinen, A., Hao, L., Yli-Pirilä, P., Kortelainen, M., Grigonyte, J., Tissari, J., Lamberg, H., Hartikainen, A., Kuuspalo, K., Kortelainen, A. M., Virtanen, A., Lehtinen, K. E. J., Komppula, M., Pieber, S., Prévôt, A. S. H., Onasch, T. B., Worsnop, D. R., Czech, H., Zimmermann, R., Jokiniemi, J., and Sippula, O.: Transformation of logwood combustion emissions in a smog chamber: Formation of secondary organic aerosol and changes in the primary organic aerosol upon daytime and nighttime aging, Atmos. Chem. Phys., 16, 13251-13269, 10.5194/acp-16-13251-2016, 2016.
Vassura, I., Venturini, E., Marchetti, S., Piazzalunga, A., Bernardi, E., Fermo, P., and Passarini, F.: Markers and influence of open biomass burning on atmospheric particulate size and composition during a major bonfire event, Atmos Environ, 82, 218-225, 10.1016/j.atmosenv.2013.10.037, 2014.
Vecchi, R., Bernardoni, V., Cricchio, D., D'Alessandro, A., Fermo, P., Lucarelli, F., Nava, S., Piazzalunga, A., and Valli, G.: The impact of fireworks on airborne particles, Atmos Environ, 42, 1121-1132, http://dx.doi.org/10.1016/j.atmosenv.2007.10.047, 2008.
Veres, P., Roberts, J. M., Burling, I. R., Warneke, C., de Gouw, J., and Yokelson, R. J.: Measurements of gas-phase inorganic and organic acids from biomass fires by negative-ion proton-transfer chemical-ionization mass spectrometry, Journal of Geophysical Research: Atmospheres, 115, n/a-n/a, 10.1029/2010jd014033, 2010.
Visser, S., Slowik, J. G., Furger, M., Zotter, P., Bukowiecki, N., Canonaco, F., Flechsig, U., Appel, K., Green, D. C., Tremper, A. H., Young, D. E., Williams, P. I., Allan, J. D., Coe, H., Williams, L. R., Mohr, C., Xu, L., Ng, N. L., Nemitz, E., Barlow, J. F., Halios, C. H., Fleming, Z. L., Baltensperger, U., and Prévôt, A. S. H.: Advanced source apportionment of size-resolved trace elements at multiple sites in london during winter, Atmos. Chem. Phys., 15, 11291-11309, 10.5194/acp-15-11291-2015, 2015.
Wang, L. W., Wen, L., Xu, C. H., Chen, J. M., Wang, X. F., Yang, L. X., Wang, W. X., Yang, X., Sui, X., Yao, L., and Zhang, Q. Z.: Hono and its potential source particulate nitrite at an urban site in north china during the cold season, Science of The Total Environment, 538, 93-101, 10.1016/j.scitotenv.2015.08.032, 2015.
Wang, Y., Zhuang, G., Xu, C., and An, Z.: The air pollution caused by the burning of fireworks during the lantern festival in beijing, Atmos Environ, 41, 417-431, http://dx.doi.org/10.1016/j.atmosenv.2006.07.043, 2007.
Washenfelder, R. A., Attwood, A. R., Brock, C. A., Guo, H., Xu, L., Weber, R. J., Ng, N. L., Allen, H. M., Ayres, B. R., Baumann, K., Cohen, R. C., Draper, D. C., Duffey, K. C., Edgerton, E., Fry, J. L., Hu, W. W., Jimenez, J. L., Palm, B. B., Romer, P., Stone, E. A., Wooldridge, P. J., and Brown, S. S.: Biomass burning dominates brown carbon absorption in the rural southeastern united states, Geophys Res Lett, 42, 653-664, 10.1002/2014gl062444, 2015.
Weingartner, E., Saathoff, H., Schnaiter, M., Streit, N., Bitnar, B., and Baltensperger, U.: Absorption of light by soot particles: Determination of the absorption coefficient by means of aethalometers, J Aerosol Sci, 34, 1445-1463, 10.1016/S0021-8502(03)00359-8, 2003.
Xu, L., Suresh, S., Guo, H., Weber, R. J., and Ng, N. L.: Aerosol characterization over the southeastern united states using high-resolution aerosol mass spectrometry: Spatial and seasonal variation of aerosol composition and sources with a focus on organic nitrates, Atmos. Chem. Phys., 15, 7307-7336, 10.5194/acp-15-7307-2015, 2015.
Young, D. E., Allan, J. D., Williams, P. I., Green, D. C., Harrison, R. M., Yin, J., Flynn, M. J., Gallagher, M. W., and Coe, H.: Investigating a two-component model of solid fuel organic aerosol in london: Processes, pm1 contributions, and seasonality, Atmos Chem Phys, 15, 2429-2443, 10.5194/acp-15-2429-2015, 2015.
Yuan, B., Liggio, J., Wentzell, J., Li, S. M., Stark, H., Roberts, J. M., Gilman, J., Lerner, B., Warneke, C., Li, R., Leithead, A., Osthoff, H. D., Wild, R., Brown, S. S., and de Gouw, J. A.: Secondary formation of nitrated phenols: Insights from observations during the uintah basin winter ozone study (ubwos) 2014, Atmos. Chem. Phys., 16, 2139-2153, 10.5194/acp-16-2139-2016, 2016.
Zhang, J. K., Cheng, M. T., Ji, D. S., Liu, Z. R., Hu, B., Sun, Y., and Wang, Y. S.: Characterization of submicron particles during biomass burning and coal combustion periods in beijing, china, Science of The Total Environment, 562, 812-821, 10.1016/j.scitotenv.2016.04.015, 2016.
Zhang, M., Wang, X., Chen, J., Cheng, T., Wang, T., Yang, X., Gong, Y., Geng, F., and Chen, C.: Physical characterization of aerosol particles during the chinese new year's firework events, Atmos Environ, 44, 5191-5198, http://dx.doi.org/10.1016/j.atmosenv.2010.08.048, 2010.

Zhu, Q., He, L. Y., Huang, X. F., Cao, L. M., Gong, Z. H., Wang, C., Zhuang, X., and Hu, M.: Atmospheric aerosol compositions and sources at two national background sites in northern and southern china, Atmos. Chem. Phys., 16, 10283-10297, 10.5194/acp-16-10283-2016, 2016.

Zotter, P., Herich, H., Gysel, M., El-Haddad, I., Zhang, Y., Močnik, G., Hüglin, C., Baltensperger, U., Szidat, S., and Prévôt, A. S. H.: Evaluation of the absorption ångström exponents for traffic and wood burning in the aethalometer-based source apportionment using radiocarbon measurements of ambient aerosol, Atmos. Chem. Phys., 17, 4229-4249, 10.5194/acp-17-4229-2017, 2017.

Appendix A: Source apportionment solution without modifying the fragmentation table.

Comment [ERV19]: Test2, moved to appendix in response of comments of both Referees.

Figure A presents results obtained with test2. Figure A.c shows mass spectra of the two chosen solutions; five sources were identified during nbf period: BBOA, HOA, COA, SVOOA and LVOOA. In the case of the bfo period six different sources were identified: BBOA, HOA, COA, factor4 which seems to be a mixed factor with a peak at m/z43 (characteristic of SVOOA) and peaks at m/z 55 and m/z 57 (characteristic of HOA), LVOOA and BBOA_1. BBOA_1 source appears to be mixed between LVOOA (peaks at m/z28 and mz44) and BBOA (peak at m/z60). We can see here, that while test2 resulted to be the best way to deconvolve OA sources compared to tests 1,3 and 4, it still shows mixing with SVOOA, LVOOA, and BBOA_1. Situation that improved when doing OA source apportionment after modifying the fragmentation table in test2_ON.

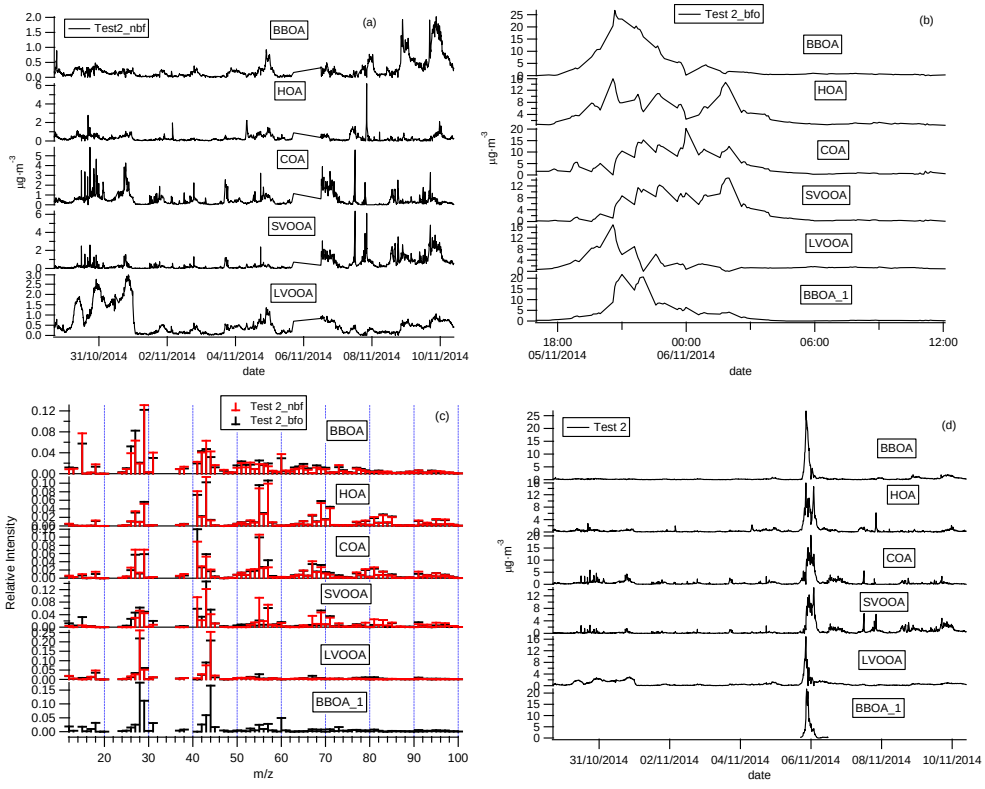

Figure A: OA sources mass spectra and time series for test 2.

Appendix B: Symbols and description of main parameters used.

Comment [ERV20]: Appendix edited changing the name of PON from Particulate Organic Nitrate to Particulate Organic Oxides of Nitrogen.

Symbol	Name
	Events
bfo	bonfire-only event (November 05-17:00 hrs – 06 - 12:00 hrs)
nbf	not bonfire (before and after bonfire night)
HSC	High secondary concentrations (October 30th to November 1st)
LC	Low concentrations (November 1st - 3rd)
WL	Winter-like (November 8th -10th)
	Aethalometer correction and model
α	Ångström absorption exponent
α_{tr}	Ångström absorption exponent for traffic
α_{wb}	Ångström absorption exponent for wood burning
ATN	Atennuation
BC	black carbon [µg.m^{-3}]
b_{abs}	absorption coefficient [m^{-1}]
b_{abs_470}	absorption coefficient at 470 nm [m^{-1}]
b_{abs_950}	absorption coefficient at 950 nm [m^{-1}]
σ_{ATN}	attenuation cross section [m^2.g^{-1}]
λ	wavelength [nm]
b_{ATN}	Uncorrected absorption coefficient [Mm^{-1}]
b_{abs}	Corrected absorption coefficient [Mm^{-1}]
C	Multiple scattering correction constant
R	Filter loading correction
f	shadowing factor
	Organic aerosol factors (OA)
BBOA	Biomass burning organic OA obtained without modifying the fragmentation table
BBOA_1	Second biomass burning organic OA obtained without modifying the fragmentation table
BBOA_2	biomass burning organic OA obtained after modifying the fragmentation table
HOA	Hydrocarbon-like OA
COA	Cooking OA
SVOOA	Semivolatile OA
LVOOA	Low volatility OA
PON	Particulate Organic Oxides of Nitrogen, calculated with 46:30 ratios.
pPON	Primary Particulate Organic Oxides of Nitrogen, estimated using the slope between PON and BBOA
sPON	Secondary Particulate Organic Oxides of Nitrogen, sPON = PON - pPON
pPON_ME2	Primary Particulate Organic Oxides of Nitrogen, calculated from ME-2 analysis
sPON_ME2	Secondary Particulate Organic Oxides of Nitrogen, calculated from ME-2 analysis

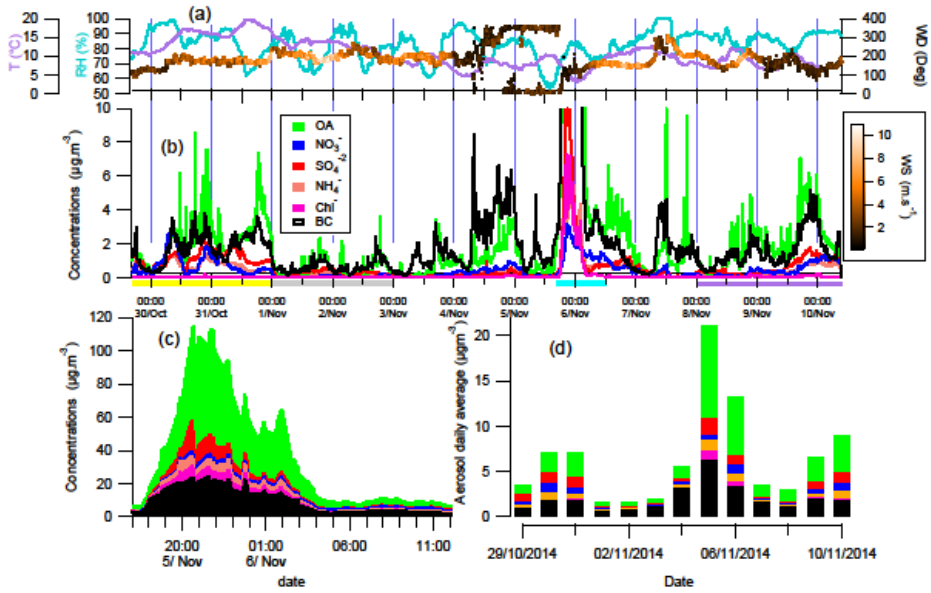

Figure 1: Meteorology (a), aerosol concentrations during all measurement period (b). Chemical component mass concentrations during bonfire night plotted cumulatively (c). Daily aerosol concentrations (d).

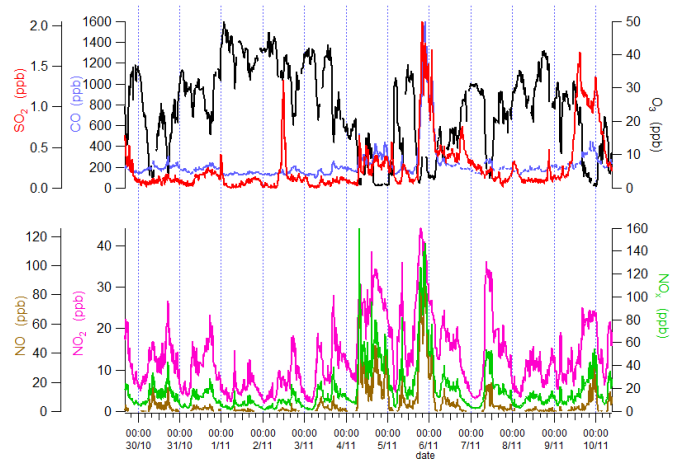

Figure 2: Time series of gases measured at Whitworth observatory.

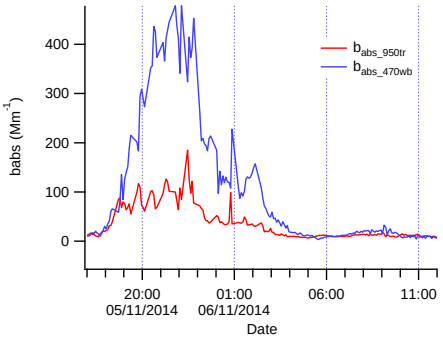

Figure 3: Absorption coefficients for Wood burning (wb) and traffic (tr).

820

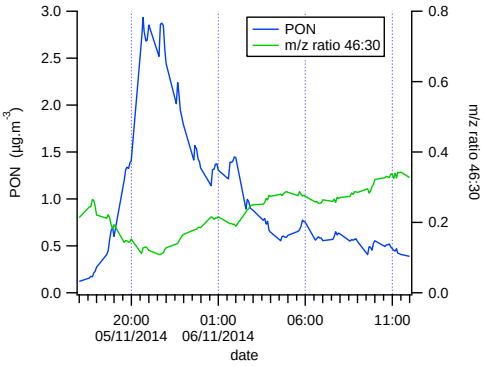

Figure 4: PON concentrations during bonfire night.

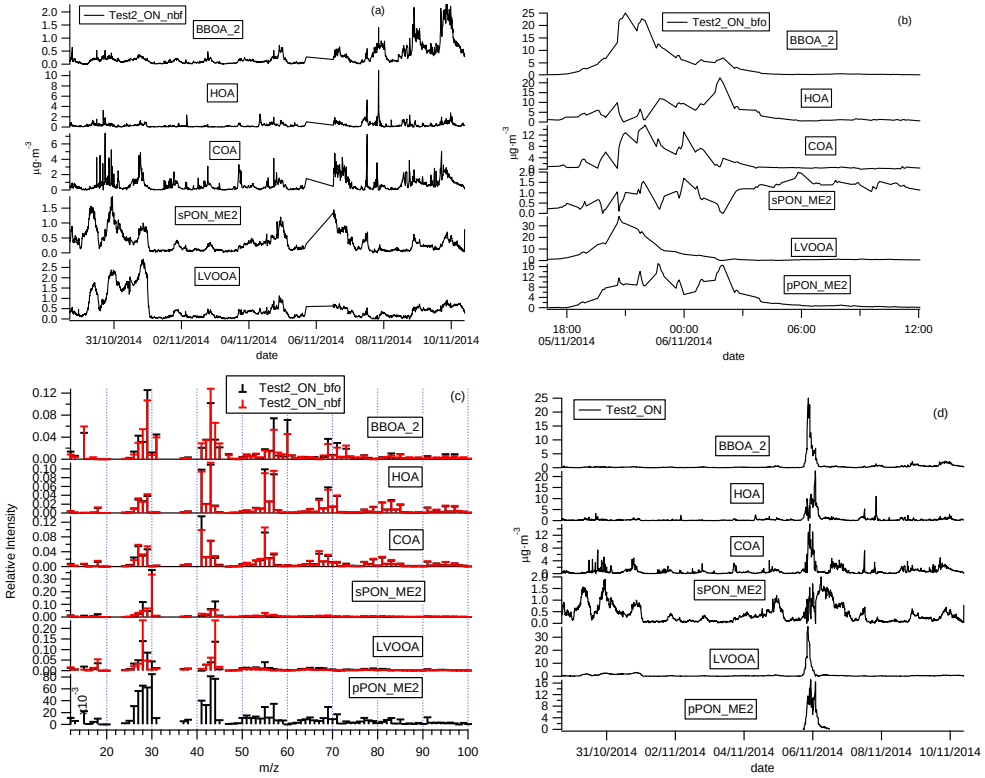

Figure 5: OA sources mass spectra and time series for test 2_ON for bonfire only (bfo) and not bonfire events (nbf). Figure 6.d shows time series of both events.

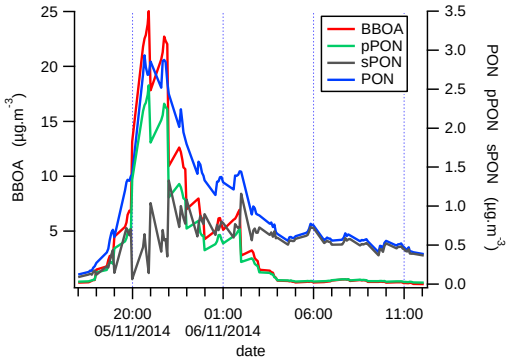

Figure 6: Secondary (sPON) and primary (pPON) organic nitrate time series estimated from PON and BBOA.

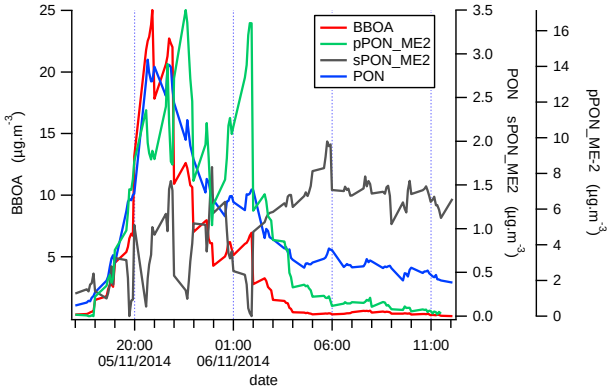

Figure 7: Secondary and primary organic nitrate time series obtained from ME-2 analysis.

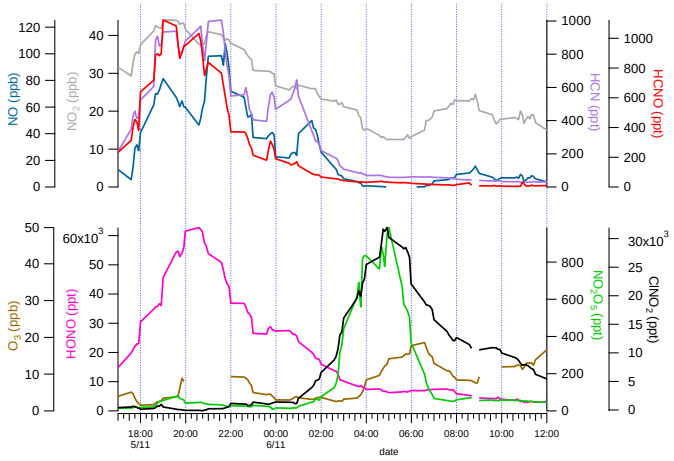

Figure 8: Time series of gases pollutants during bonfire night.

Table 1: Multilinear and linear regression analysis between b_{abs_470wb} and organic aerosols.

			All	HSC	LC	bfo	WL
MLR 1	A	bkgrd	0.000	4.555	1.004	0.000	1.293
	B	babs:BBOA	14.340	3.547	18.284	11.926	10.318
	C	babs:PON	54.495	9.212	12.046	73.115	21.724
		B/C	0.263	0.385	1.518	0.163	0.475
		r^2_MLR	0.912	0.064	0.364	0.898	0.760
Linear 1	r^2	babs:BBOA	0.861	0.043	0.358	0.839	0.739
	r^2	babs:PON	0.819	0.060	0.275	0.897	0.311
MLR 2	A	bkgrd	0.000	2.527	0.753	0.000	0.079
	B	babs:BBOA_2	15.653	27.288	26.481	14.319	10.018
	C	babs:PON	42.840	0.000	1.200	54.353	18.982
		B/C	0.365	***	22.060	0.263	0.528
		r^2_MLR	0.922	0.392	0.480	0.902	0.804
Linear 2	r^2	babs:BBOA_2	0.894	0.392	0.480	0.880	0.788
	r^2	babs:PON	0.819	0.060	0.275	0.897	0.311

			All	HSC	*HSC	LC	*bfo	WL
MLR 3	A	bkgrd	0.000	2.527	1.649	0.763	6.093	0.000
	B	babs:BBOA_2	21.545	27.288	22.764	26.668	16.657	8.577
	C	babs:sPON_ME2	3.926	0.000	0.000	0.191	0.000	9.017
	D	D			1.138		7.357	
		B/C	5.488	***	***	***	***	0.951
		B/D			20.005		2.264	
		r^2_MLR	0.896	0.392	0.418	0.480	0.910	0.803
Linear 3	r^2	babs:BBOA_2	0.894	0.392	0.392	0.480	0.880	0.788
	r^2	babs:sPON_ME2	0.024	0.000	0.000	0.273	0.188	0.647
	r^2	D			0.225		0.633	

*Trilinear regression was performed as in *bfo analysis there were two PON factors from ME-2 analysis; pPON and sPON, with D= slope babs:pPON, r^2_D = r^2 babs:pPON. In *HSC analysis; BBOA, sPON and LVOOA were used, with D= slope babs:LVOOA, r^2_D = r^2 babs:LVOOA. PON is the particulate organic nitrate estimate from 46:30 ratios. All= complete dataset; HSC= Episode with high secondary concentrations (October 30th to November 1st), LC = Episode with low concentrations (November 1st - 3rd); bfo = epidose with bonfire only concentrations (05-Nov 17:00 hrs – 06-Nov 12:00 hrs); WL= Episode with winter-like carachteristics (November 8th -10th).